



University of Kentucky
UKnowledge

University of Kentucky Master's Theses

Graduate School

2005

EXPERIMENTAL AND ANALYTICAL STUDY OF FRICTION STIR PROCESSING

Basil M. Darras

University of Kentucky, bmdarr0@engr.uky.edu

[Right click to open a feedback form in a new tab to let us know how this document benefits you.](#)

Recommended Citation

Darras, Basil M., "EXPERIMENTAL AND ANALYTICAL STUDY OF FRICTION STIR PROCESSING" (2005).
University of Kentucky Master's Theses. 353.
https://uknowledge.uky.edu/gradschool_theses/353

This Thesis is brought to you for free and open access by the Graduate School at UKnowledge. It has been accepted for inclusion in University of Kentucky Master's Theses by an authorized administrator of UKnowledge. For more information, please contact UKnowledge@lsv.uky.edu.

ABSTRACT OF THESIS

EXPERIMENTAL AND ANALYTICAL STUDY OF FRICTION STIR PROCESSING

Friction stir processing (FSP) has recently become an effective microstructural modifications technique. Reported results showed that for different alloys, FSP produces very fine equiaxed and homogeneous grain structure. FSP is considered to be a new processing technique and more experimental and analytical investigations are needed to advance the industrial utilization of FSP. Most of the work that has been done in the friction stir processing field is experimental and limited modeling activities have been conducted. Attempts to develop a predictive model to correlate the resulting microstructure with process parameters are scarce.

In this work, commercial 5052 Aluminum alloy sheets are friction stir processed at different rotational and translational speeds. The effects of process parameters on the resulting microstructure and mechanical properties are investigated. The results show that FSP produces very fine and homogenous grain structure, and it is observed that smaller grain size structure is obtained at lower rotational speeds. It is also observed that the hardness of the processed sheet depends strongly on the rotational and translational speeds and varies widely within the processed region. The results suggest that the temperature achieved during processing plays an important role in determining the microstructure and properties of the processed sheet. In addition, a new modeling approach based on experiments and theory is proposed to predict the grain size of the friction stir processed material as a function of process parameters. The proposed approach involves determination of the strain rate distribution in the processed (deformation) zone based on the velocity fields of the material and correlating the strain rate distribution with the average grain size of the resulting microstructure using Zener-Holloman parameter.

Keywords: Friction Stir Processing, Microstructure, Hardness, Modeling, AA5052

Basil M. Darras

Date: 11/10/2005

EXPERIMENTAL AND ANALYTICAL STUDY OF FRICTION STIR PROCESSING

By

Basil M. Darras

Dr. Marwan Khraisheh

(Director of Thesis)

Dr. George Huang

(Director of Graduate Studies)

Date: 11/10/2005

RULES FOR THE USE OF THESIS

Unpublished thesis submitted for the Master's degree and deposited in the University of Kentucky Library are as a rule open for inspection, but are to be used only with due regard to the rights of the authors. Bibliographical references may be noted, but quotations or summaries of parts may be published only with the permission of the author, and with the usual scholarly acknowledgements.

Extensive copying or publication of the thesis in whole or in part also requires the consent of the Dean of the Graduate School of the University of Kentucky.

THESIS

Basil M. Darras

The Graduate School
University of Kentucky

2005

EXPERIMENTAL AND ANALYTICAL STUDY OF FRICTION STIR PROCESSING

THESIS

A thesis submitted in partial fulfillment of the requirements
for the degree of Master of Science in the
College of Engineering at the
University of Kentucky

By

Basil M. Darras

Lexington, Kentucky

Director: Dr. Marwan Khraisheh

(Associate Professor of Mechanical Engineering)

Lexington, Kentucky

2005

ACKNOWLEDGMENTS

Firstly I would like to thank my advisor, Dr. Marwan Khraisheh for his continuous support, mentoring, advising, and guidance extended throughout my MS. Also I would like to thank Dr. Jawahir, who has been very encouraging and supportive all through my M.S. and also for his kindness in agreeing to be on my committee. I would then like to extend my thankfulness to Dr. Badurdeen, for agreeing to be on my committee. Also I would like to thank my D.G.S. Dr. Huang, for giving me an opportunity to pursue my MS at University of Kentucky. I would like to express my sincere gratitude to Mr. VonKuster for his technical support and guidance through out the course of the experiments. Also I would like to thank my research team members and my friends, with whom I've shared and discussed this project in several versions. Their help, advice, and support have been vital throughout. Above all, I would like to thank my parents, brothers and sisters for their continuous support and motivation.

CONTENTS

ACKNOWLEDGMENTS.....	iii
CONTENTS	iv
LIST OF TABLES.....	vi
LIST OF FIGURES.....	vii
CH-1 INTRODUCTION.....	1
1.1 Motivation	1
1.2 Research objectives	2
1.3 Thesis layout	3
CH-2 BACKGROUND	4
2.1 Friction stir welding (FSW)	4
2.2 Principle of friction stir processing	6
2.3 Significance of friction stir processing.....	8
2.4 Previous works.....	10
<i>2.4-1 Microstructure and mechanical properties</i>	<i>10</i>
<i>2.4-2 Superplasticity</i>	<i>16</i>
<i>2.4-3 Modeling:</i>	<i>20</i>
CH-3 EXPERIMENTAL INVESTIGATION.....	34
3.1 Material	34
3.2 Experimental setup.....	34
<i>3.2-1 Experimental procedure</i>	<i>36</i>
<i>3.2-2 Microstructural investigation</i>	<i>38</i>
<i>3.2-2 Hardness testing</i>	<i>39</i>
3.3 Results	40
<i>3.3-1 Grain structure</i>	<i>40</i>
<i>3.3-2 Hardness.....</i>	<i>43</i>
<i>3.3-3 FS processed quality</i>	<i>47</i>
CH-4 MODELING OF FRICTION STIR PROCESS	50
4.1 Modeling approach.....	51
<i>4.1-1 Assumptions</i>	<i>51</i>
<i>4.1-2 Deformation zone</i>	<i>53</i>
<i>4.1-3 Contact state variable.....</i>	<i>54</i>
<i>4.1-4 Velocity fields</i>	<i>55</i>
<i>4.1-5 Strain rate fields</i>	<i>57</i>

<i>4.1-6 Effective strain rate</i>	58
<i>4.1-7 Zener-Holloman parameter</i>	58
4.2 Preliminary results	59
CH-5 SUMMARY AND FUTURE WORKS	65
5.1 Future work	66
REFERENCES	68
VITA	73

LIST OF TABLES

TABLE 3- 1 COMPOSITIONS OF ALUMINUM ALLOY 5052 (WT %) [34].....	34
TABLE 3- 2 SAMPLES FS PROCESSED AT DIFFERENT PROCESS PARAMETERS	39
TABLE 3- 3 FS PROCESSED AA5052 SHEET AT DIFFERENT ROTATIONAL SPEED	48
TABLE 3- 4 FS PROCESSED AA5052 SHEET AT DIFFERENT TRANSLATIONAL SPEED	49

LIST OF FIGURES

FIGURE 2- 1 SCHEMATIC OF FRICTION STIR WELDING (FSW).....	5
FIGURE 2- 2 SCHEMATIC FOR FRICTION STIR PROCESSING (FSP) [11]	7
FIGURE 2- 3 SCHEMATICS OF THE STAGES OF FRICTION STIR PROCESSING (FSP) ...	7
FIGURE 2- 4 GRAIN SIZE EFFECT ON AL 7475 SUPERPLASTIC ALLOY.....	9
FIGURE 2- 5 CHARACTERISTIC CURVE OF SUPERPLASTIC MATERIAL SHOWING THE EFFECT OF USING FINE GRAIN STRUCTURE	9
FIGURE 2- 6 GRAIN STRUCTURES IN TOP REGION OF THE PROCESSING NUGGET. (A) DISLOCATION FREE GRAIN, (B) GRAIN WITH LOW DENSITY OF DISLOCATION, (C) GRAIN WITH HIGH DENSITY OF DISLOCATION AND (D) RECOVERY STRUCTURE. [4].....	11
FIGURE 2- 7 MICROSTRUCTURE AS A FUNCTION OF TRANSVERSE AND THROUGH- THICKNESS LOCATIONS [6]	13
FIGURE 2- 8 COMPARISON OF ROOM TEMPERATURE AND LOW-TEMPERATURE FSW MICROSTRUCTURES IN 2024 AL WITH THE BASE METAL MICROSTRUCTURES. (A) LIGHT METALLOGRAPHIC VIEW OF BASE METAL. (B) TEM VIEW OF BASE METAL. (C) TEM VIEW OF ROOM-TEMPERATURE WELD ZONE CENTER. (D) TEM VIEW OF LOW-TEMPERATURE WELD ZONE CENTER. NOTE DENSE DISLOCATION DENSITY IN (B) IN CONTRAST TO (C) AND (D) [10]	14
FIGURE 2- 9 AVERAGE HARDNESS AND TENSILE STRENGTH FOR UNPROCESSED ZONE AND FRICTION STIR ZONE AT DIFFERENT TOOL ROTATIONAL SPEED [10].....	15
FIGURE 2- 10 UNPROCESSED AA5052 SHEET (A, OPTICAL MICROSCOPE), FS PROCESSED ZONE AT 600RPM, 2.5IN/MIN. (B, TEM), AND FS PROCESSED ZONE AT 800, 2.5IN/MIN. (C, TEM). [11].....	15
FIGURE 2- 11 MICROSTRUCTURE OF 7075 AL ALLOY A) AS RECEIVED AND B) FSP [12].....	16
FIGURE 2- 12 ELONGATION VERSUS TEMPERATURE PLOTS AT INITIAL STRAIN RATE OF 10 ⁻² S ⁻¹ FOR THE NINE PASS FSP ALLOY [12].....	17
FIGURE 2- 13 STRESS-STRAIN BEHAVIOR OF FSP A356 AS A FUNCTION OF A) INITIAL STRAIN RATE AT 530 °C AND B) TEMPERATURE AT AN INITIAL STRAIN RATE OF 1X10 ⁻³ S ⁻¹ [13].	17
FIGURE 2- 14 VARIATION OF ELONGATION WITH A) INITIAL STRAIN RATE AND B) TEMPERATURE FOR BOTH FSP AND CAST A356 [13].....	18
FIGURE 2- 15 THREE CUPS PUNCH FORMED AT 723 K: (A) AS-RECEIVED; (B) FSP AT 18.5MM PUNCH STROKE; (C) FSP AT 28.5MM PUNCH STROKE. [17]	19
FIGURE 2- 16 STIR WELDING TEMPERATURE AS A FUNCTION OF (A) ROTATIONAL SPEED AND (B) WELDING SPEED [18].....	21
FIGURE 2- 17 TEMPERATURE PROFILE AT 8.2 RE/S AND 1.4 MM/S [18].....	21
FIGURE 2- 18 VARIATIONS OF THE (A) STRAIN RATE (B) TEMPERATURE AND (C) THE AVERAGE GRAIN SIZE AS A FUNCTION OF PIN ROTATION SPEED [19].....	23
FIGURE 2- 19 METAL FLOW PATTERNS DURING FRICTION STIR JOINING [23]	26
FIGURE 2- 20 MATERIAL FLOW FIELDS IN FRICTION STIR WELDS [24]	28
FIGURE 2- 21 COMPARISON BETWEEN THE MEASURED AND THE CALCULATED AVERAGE GRAIN SIZES (FEW6-715 RPM, 71.5 MM/MIN, AND DEPTH 2.5 MM) [26]	31

FIGURE 3- 1 DIFFERENT TOOL CONFIGURATIONS	35
FIGURE 3- 2 ASSEMBLY OF BACKING PLATE HOLDING PLATES AND SAMPLE	35
FIGURE 3- 3 HAAS VF-0F CNC VERTICAL MILLING MACHINE	36
FIGURE 3- 4 EXPERIMENTAL SETUP	36
FIGURE 3- 5 SCHEMATICS OF THE STAGES OF FRICTION STIR PROCESSING (FSP) .	37
FIGURE 3- 6 SCHEMATIC OF THE PREPARED SAMPLES	38
FIGURE 3- 7 THE GRAIN STRUCTURE AT DIFFERENT LOCATIONS OF THE FS PROCESSED AA5052 SHEET, AT DIFFERENT CONDITIONS USING OIM. (<i>IN COLLABORATION WITH DEPARTMENT OF MECHANICAL ENGINEERING, FAMU- FSU</i>).....	40
FIGURE 3- 8 AVERAGE GRAIN SIZE COMPARISON OF AS RECEIVED SAMPLE AND FS PROCESSED AT DIFFERENT PROCESS PARAMETERS COMBINATIONS. (<i>IN COLLABORATION WITH DEPARTMENT OF MECHANICAL ENGINEERING, FAMU- FSU</i>).....	41
FIGURE 3- 9 THE ORIENTATION IMAGING MICROSCOPY MAP OF (A) AS RECEIVED AA5052 SAMPLE, (B) FSP AT 1000 RPM AND 2.5 IN/MIN (SAMPLE B2), (C) FSP AT 1000 RPM AND 2.0 IN/MIN (SAMPLE A2)AND (C) FSP AT 600 AND 2.5 IN/MIN (SAMPLE B1) (<i>IN COLLABORATION WITH DEPARTMENT OF MECHANICAL ENGINEERING, FAMU-FSU</i>)	42
FIGURE 3- 10 THE AVERAGE GRAIN MISORIENTATION FOR; (A) AS RECEIVED SAMPLE, (B) FSP AT 600 RPM AND 2.5 IN/MIN (SAMPLE B1) (<i>IN COLLABORATION WITH DEPARTMENT OF MECHANICAL ENGINEERING, FAMU-FSU</i>).....	43
FIGURE 3- 11 AVERAGE HARDNESS (HV) OF FS PROCESSED AT DIFFERENT ROTATIONAL SPEED (TRANSLATIONAL SPEED IS 2.0 IN/MIN.).....	44
FIGURE 3- 12 AVERAGE HARDNESS (HV) OF FS PROCESSED AT DIFFERENT TRANSLATIONAL SPEED (ROTATIONAL SPEED IS 500 RPM)	44
FIGURE 3- 13 AVERAGE HARDNESS (HV) OF FS PROCESSED AT DIFFERENT LONGITUDINAL POSITIONS (FS PROCESSED AT 500 RPM AND 2 IN/MIN.)	45
FIGURE 3- 14 AVERAGE HARDNESS (HV) OF FS PROCESSED AT DIFFERENT POSITIONS WITHIN THE (FS PROCESSED AT 500 RPM AND 2 IN/MIN.)	46
FIGURE 3- 15 AVERAGE HARDNESS (HV) OF FS PROCESSED AT DIFFERENT TRANSVERS POSITIONS (FS PROCESSED AT 500 RPM AND 2 IN/MIN.).....	47
FIGURE 4- 1 MODEL FLOW CHART	52
FIGURE 4- 2 SCHEMATIC OF FSP DEFORMATION ZONE.....	53
FIGURE 4- 3 THE EFFECT OF ROTATIONAL SPEED ON THE EFFECTIVE STRAIN RATE (A) RESULT FROM THE PROPOSED MODEL AND (B) RESULT FROM LITERATURE [18].....	60
FIGURE 4- 4 THE EFFECT OF TRANSLATIONAL SPEED ON THE EFFECTIVE STRAIN RATE (MODELING RESULTS).....	61
FIGURE 4- 5 THE VARIATION OF EFFECTIVE STRAIN RATE WITH THE DISTANCE FROM THE CENTER OF THE TOOL (MODELING RESULTS).....	61
FIGURE 4- 6 THE VARIATION OF EFFECTIVE STRAIN RATE WITH THE ANGLE (MODELING RESULTS).....	62
FIGURE 4- 7 THE VARIATION OF EFFECTIVE STRAIN RATE WITH THE DEPTH WITHIN THE SHEET THICKNESS (MODELING RESULTS).....	62
FIGURE 4- 8 THE STRAIN RATE DISTRIBUTIONS WITHIN THE DEFORMATION ZONE AT 400 RPM AND 2.0 IN/MIN. (MODELING RESULTS USING MATLAB).....	63
FIGURE 4- 9 THE STRAIN RATE DISTRIBUTIONS WITHIN THE DEFORMATION ZONE AT 600 RPM AND 2.0 IN/MIN. (MODELING RESULTS USING MATLAB).....	63

FIGURE 4- 10 THE STRAIN RATE DISTRIBUTIONS WITHIN THE DEFORMATION ZONE
AT 800 RPM AND 2.0 IN/MIN. (MODELING RESULTS USING MATLAB)..... 64

FIGURE 4- 11 THE STRAIN RATE DISTRIBUTIONS WITHIN THE DEFORMATION
ZONE AT 600 RPM AND 4.0 IN/MIN. (MODELING RESULTS USING MATLAB)... 64

CHAPTER-1 INTRODUCTION

Friction stir processing (FSP) is a new microstructural modifications technique; recently it FSP has become an efficient tool for homogenizing and refining the grain structure of metal sheet. Friction stir processing is believed to have a great potential in the field of superplasticity. Results have been reported that FSP greatly enhances superplasticity in many Al alloy [12-17]. Friction stir processing is based on friction stir welding (FSW) which was invented by The Welding Institute (TWI) of United Kingdom in 1991 [1, 2].

Friction stir processing (FSP) is a solid-state process which means that at any time of the processing the material is in the solid state. In FSP a specially designed rotating cylindrical tool that comprises of a pin and shoulder that have dimensions proportional to the sheet thickness. The pin of the rotating tool is plunged into the sheet material and the shoulder comes into contact with the surface of the sheet, and then traverses in the desired direction. The contact between the rotating tool and the sheet generate heat which softens the material below the melting point of the sheet and with the mechanical stirring caused by the pin, the material within the processed zone undergoes intense plastic deformation yielding a dynamically-recrystallized fine grain microstructure.

1.1 Motivation

Forming and Formability of light weight alloys at room temperatures for aerospace and automotive applications present a major challenge. One way to improve the formability is to refine and homogenize the microstructure and form the sheet at high temperatures using advanced forming techniques such as superplastic forming. Recent observations have indicated that ultrafine grain sheet metals have superior formability at relatively moderate temperatures. However, the difficulty in producing ultrafine grain sheet metals hinders the widespread utilization of light weight alloys in the transportation industry. Conventional grain refinement techniques usually involve thermo-mechanical

processing (e.g. hot rolling) which is costly, time consuming, and negatively affects the environment due to high energy consumption. Alternative effective grain refinement methods are very much needed.

As the concept of FSP being relatively new, there are many areas, which need thorough investigation to optimize the process and make it commercially viable. In order to obtain the desired finer grain size, certain process parameters like rotational and translation speeds, tool geometry etc., are to be controlled. Several investigations are being carried out in order to study the effects of these process parameters on the grain structure. Another important field that need to be worked on is developing predictive models or tools that can predicate microstructure and properties of the processed material so that one can choose the suitable process parameters to achieve the desire microstructure modification, and optimize the process.

1.2 Research objectives

The aim of this work is to study friction stir processing as a microstructural modification technique. Investigations of microstructure, mechanical behavior of the friction stir processed material. And to achieve that, the following specific objectives are achieved:

- a) To design an experimental setup to conduct friction stir processing
- b) Investigate the effects of rotational and translational speeds on the resulting microstructure of the friction processed material
- c) Investigate the effect of FSP on the resulting hardness of the FS processed material.
- d) To develop a new physics-based model based on theory and experiments, to predict the resulting grain size from the process parameters

1.3 Thesis layout

The thesis consists of five chapters. The first chapter gives a brief introduction about friction stir processing, motivations and research objectives. In Chapter 2 general background about friction stir welding, the idea and the principle of friction stir processing and a detailed literature review are presented. Experimental investigations are explained in Chapter 3, the experimental setup and the methodologies used to conduct the experiments are explained, and microstructural results are presented and discussed in this chapter. Chapter 4 provides the modeling part of this work. A brief introduction about thermal, mechanical and microstructural modeling is presented, and then a new modeling approach is introduced, detailed modeling procedures are explained and finally preliminary modeling results are discussed. The last chapter (Chapter 5) summarizes the work that has been done and finished with final remarks and future work.

CHAPTER-2 BACKGROUND

Friction stir processing (FSP) is a new microstructure modification technique, which is based on the friction stir welding (FSW) which was invented by The Welding Institute (TWI) of United Kingdom in 1991 [1, 2]. FSP has recently become an efficient tool of homogenizing and refining of the grain structure of metal. Therefore, it has a great potential in the field of superplasticity. It has been reported that FSP greatly enhances superplasticity in many Al alloys [12-17].

This chapter presents a general introduction about friction stir welding (FSW) and friction stir processing (FSP), their principle and the significance. In addition, a detailed literature review that covers microstructure, mechanical properties, superplasticity and modeling of friction stir are given.

2.1 Friction stir welding (FSW)

Friction stir welding was invented by TWI, Cambridge in 1991 [1, 2]. Friction stir welding involves the joining of metals without fusion or filler materials; it produces a plasticized region of material. A non-consumable rotating tool is pushed into the materials to be welded and then the central pin, followed by the shoulder, is brought into contact with the two parts to be joined as shown in Figure 2-1. The rotation of the tool heats up and plasticizes the materials it is in contact with and as the tool moves along the joint line, the material from the front of the tool is swept around this plasticized annulus to the rear, eliminating the interface. So the welds are created by the combined action of frictional heating and mechanical deformation due to a rotating tool. The maximum temperature reached is of the order of 0.8 of the melting temperature. The tool has a circular section except at the end where there is a threaded probe or more complicated flute; the junction between the cylindrical portion and the probe is known as the shoulder. The pin penetrates the workpiece whereas the shoulder rubs with the top surface. The heat is generated primarily by friction between a rotating-translating tool and the

workpiece, the shoulder of which rubs against the workpiece. There is a volumetric contribution to heat generation from the adiabatic heating due to deformation near the pin. The welding parameters have to be adjusted so that the ratio of frictional to volumetric deformation induced heating decreases as the workpiece becomes thicker. This is in order to ensure a sufficient heat input per unit length.

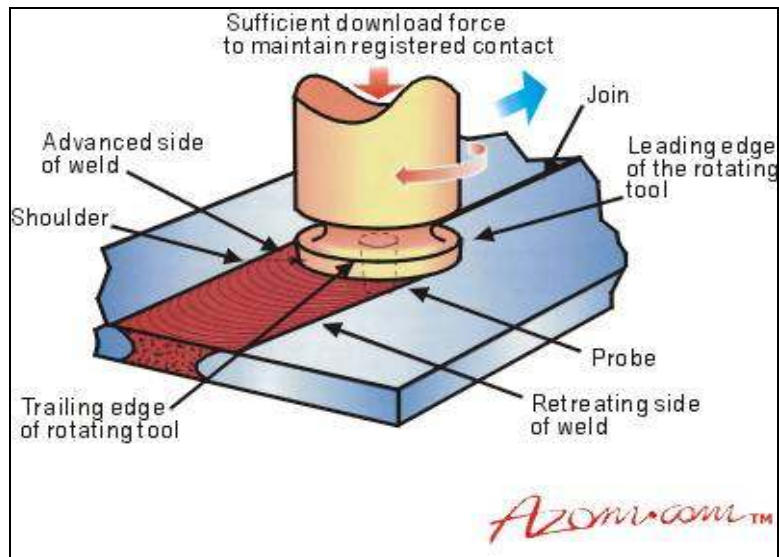


Figure 2- 1 Schematic of friction stir welding (FSW)

Friction stir welding is used already in routine, as well as critical applications, because it produces strong and ductile joints. The process is most suitable for components which are flat and long (plates and sheets) but also it can be used for pipes, hollow sections, and positional welding.

Traditionally, friction welding is carried out by moving one component relative to the other along a common interface, while applying a compressive force across the joint. The friction heating generated at the interface softens both components, and when they become plasticized the interface material is extruded out of the edges of the joint so that clean material from each component is left along the original interface. The relative motion is then stopped, and a higher final compressive force may be applied before the joint is allowed to cool down. The key to friction welding is that no molten material is generated, the weld being formed in the solid state. The friction heating is generated

locally, so there is no widespread softening of the assembly. Friction welding has gained much interest among researchers and also in many industries because of the following advantages:

- The weld is formed across the entire cross-sectional area of the interface in a single shot process
- The technique is capable of joining dissimilar materials with different melting temperatures and physical properties.
- The process is completed in a few seconds with very high reproducibility - an essential requirement for a mass production industry.
- The process is environmentally friendly.
- This technique does not require consumables (filler wire, flux or gas) and produces no fumes

The principles of this method now form the basis of many types of friction welding. Some of the friction stir techniques are; rotary friction welding, linear friction welding, radial friction welding, friction plunge welding without containment shoulder, and friction stir welding which is studied in this work [3].

2.2 Principle of friction stir processing

To friction stir process a sheet a specially designed cylindrical tool is used, the tool consists of a pin and a concentric larger diameter shoulder as shown in Figure 2-2. While the tool is rotating the pin is plunged into the sheet and the shoulder comes in contact with the surface of the sheet. The friction between the tool and the sheet generates heat which softens the material without reaching the melting temperature of the material; that is why it is a solid state process. Then the tool is transverse in the desired direction while it is rotating. The rotation of the pin does the stirring action of the softened material which makes the material undergo intense plastic deformation yielding a dynamically recrystallized fine, equiaxed, and defect free grain structure.

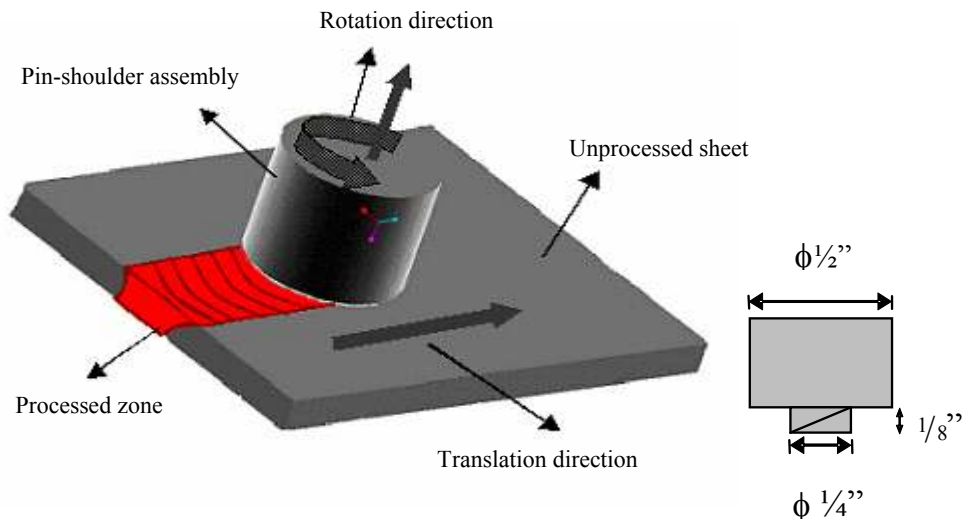


Figure 2- 2 Schematic for friction stir processing (FSP) [11]

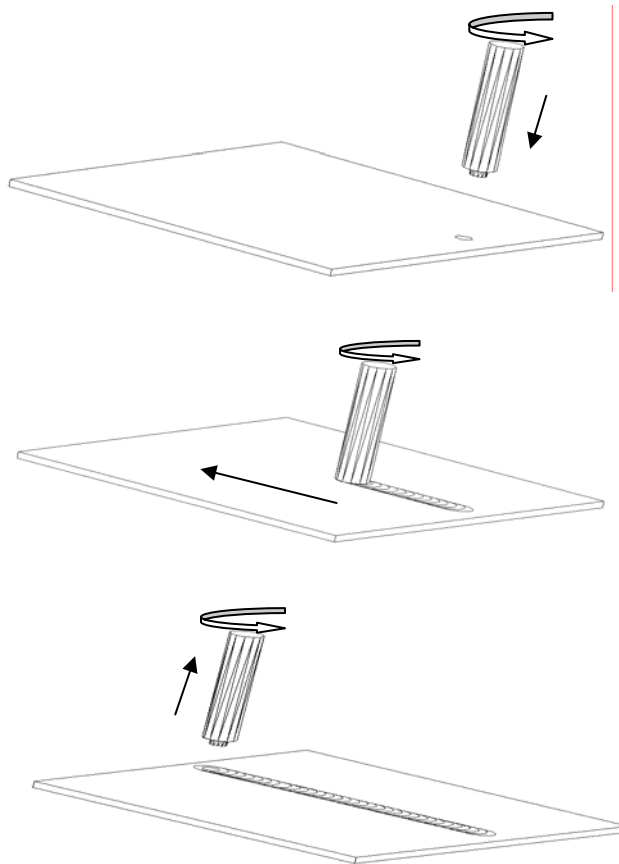


Figure 2- 3 Schematics of the stages of friction stir processing (FSP)

2.3 Significance of friction stir processing

Finding a material with specific properties is one of the most important issues in many industrial applications, especially in the aerospace and transportation industries. So there is a need of designing material with the desired properties. However, there are many limitations in terms of cost and time of production with conventional processing techniques. High strength accompanied by high ductility is possible with materials having fine and homogenous grain structures. There are different processing techniques that would produce a material with small grain size that satisfies the requirements of strength and ductility. New processing techniques like Friction Stir Processing (FSP), Equal Channel Angular Extrusion (ECAE), are being developed for this purpose in addition to the improvements in conventional processing techniques like the Rockwell process, and the powder metallurgy technique.

One of the potential applications of FSP is the forming and formability of light weight alloys at room temperatures for aerospace and automotive applications which present a major challenge. One way to improve the formability is to refine and homogenize the microstructure and form the sheet at high temperatures using advanced forming techniques such as superplastic forming. Recent observations have indicated that fine grain structure sheet metals have superior formability at relatively moderate temperatures as indicated in Figure 2-4. It is known that as the grain size decreases the strain rate sensitivity (m) increases and the optimum strain rate also increases which mean enhancing the superplasticity at lower temperature as indicated in Figure 2-5. However, the difficulty in producing ultrafine grain sheet metals hinders the widespread utilization of light weight alloys in the transportation industry.

Conventional grain refinement techniques usually involve thermo-mechanical processing (e.g. hot rolling) which is costly, time consuming, and negatively affects the environment due to high energy consumption. Alternative effective grain refinement methods are very much needed. Recently, a new process based on Friction Stir Welding (FSW) has been found to produce fine-grained microstructure. Friction Stir Processing (FSP) can be used to effectively produce ultrafine grain and homogenized structure.

During FSP, a specially designed cylindrical tool is plunged into the sheet causing intense plastic deformation through stirring action, yielding a defect free, and dynamically recrystallized, fine grain microstructure.

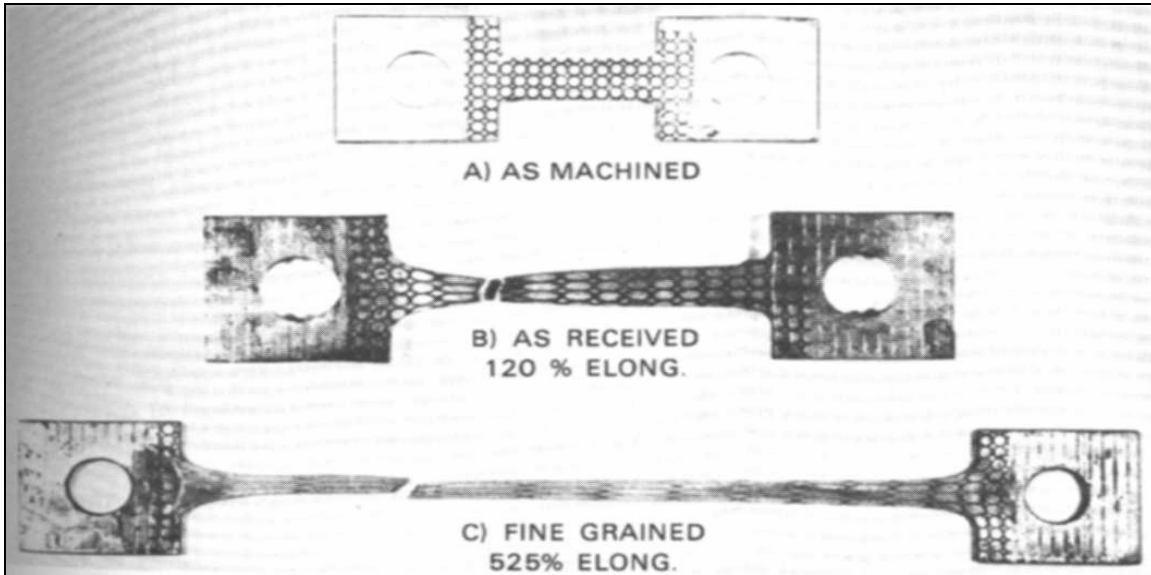


Figure 2- 4 Grain Size Effect on Al 7475 Superplastic Alloy

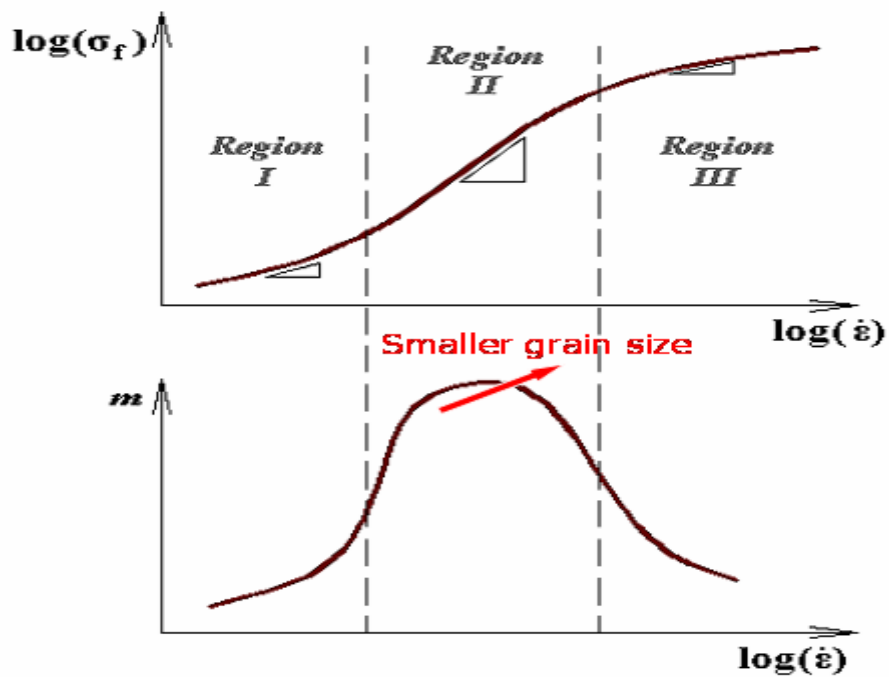


Figure 2- 5 Characteristic curve of superplastic material showing the effect of using fine grain structure

Friction stir processing offers many advantages over conventional and other newer material processing techniques. One of the most important and unique features of FSP is that FSP is a single step process, while other techniques require multiple steps which make FSP easier and less time consuming. In addition, FSP uses a simple inexpensive tool, and a readily available machine such as a milling machine can be used to conduct the process. Other advantages of FSP are that it is suitable for automation, and it is also environmentally friendly since no gases or chemical are used. These features together make FSP easier and less expensive and so preferable over other processing techniques. However, there are some limitations that need to be eliminated by intensive research. Since FSP is a new technique the most important issue is the availability of data. Another obstacle is the lack of predictive models for the resulting microstructure. With respect to the process itself; the keyhole at the end of each pass and the need of a backing plate are among the major issues that need to be solved.

2.4 Previous works

Friction stir processing and welding are recent technologies. FSW was invented in 1991 by TWI in United Kingdom [1, 2]. The first work that been published in friction stir processing was in 1998. Since then many researchers have investigated different aspects of the processes, such as microstructure, mechanical properties, superplasticity of FSP, forces generated, and mechanical and thermal modeling works.

This section gives a detailed literature review about microstructure and mechanical properties, as well as superplasticity of FSP and the modeling works that been done in this area.

2.4-1 Microstructure and mechanical properties

Most of the work done in the field of friction stir welding and processing focused on investigating the effect of the process parameters on the microstructure and mechanical properties of the material. Microstructural investigations using different techniques such as optical microscopy, Transmission Electron Microscopy (TEM), Scanning Electron Microscopy (SEM), and Orientation Imaging microscopy (OIM) were

done. Mechanical properties were also investigated by applying several mechanical testing; such as tensile test, hardness test, microhardness test, etc..

Su et al. [4] studied the resulting microstructure of friction stir processed commercial 7075 Al alloy. The grain structure of FS processed area was examined by TEM. Su et al. observed that the microstructure of FS processed area did not have a uniform grain size distribution. The average grain size slightly decreases from top to bottom. Also diffraction rings were observed which, according to them confirm that there are large misorientations between the individual grains. Generally the dislocation density was not uniform within the stir zone even with similar grain size; this observation suggested that non-uniform plastic deformation was introduced in the recrystallized grains during FSP. By running multiple overlapping passes any desired sheet size can be processed to an ultrafine grained microstructure. The investigations showed that multiple overlapping passes indicated can be used as an effective technique to fabricate large bulk ultrafine grain material with relatively uniform microstructure.

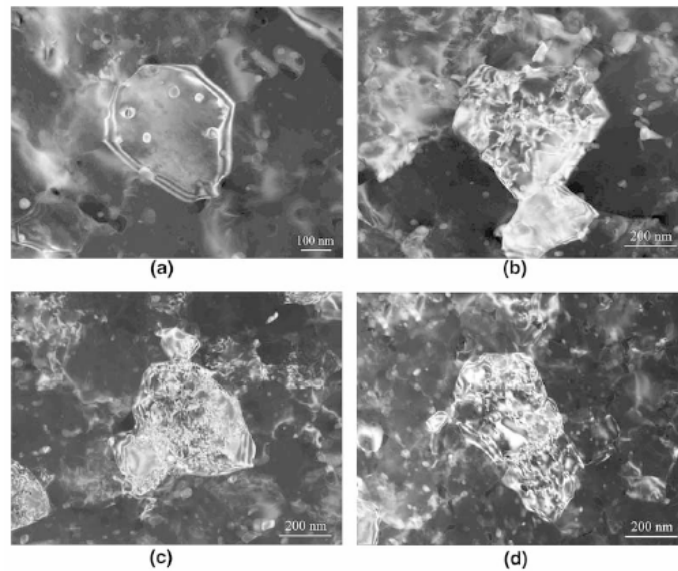


Figure 2- 6 Grain structures in top region of the processing nugget. (a) Dislocation free grain, (b) grain with low density of dislocation, (c) grain with high density of dislocation and (d) recovery structure. [4]

Peel et al. [5] reported the results of microstructural, mechanical property and residual stress investigations of AA5083 FS welds. According to them the weld properties were dominated by the thermal input rather than the mechanical deformation caused by the tool. Their results showed that increasing the traverse speed and hence reducing the heat input narrowed weld zone, also that the recrystallization in the weld zone had considerably lower hardness and yield stress than the parent AA5083. It was observed that almost all the plastic flow occurred within the recrystallized weld zone and the synchrotron residual stress analysis indicated that the weld zone is in tension in both the longitudinal and transverse directions. The peak longitudinal stresses increased as the traverse speed increases. They suggested that this increase is probably due to steeper thermal gradients during welding and the reduced time for stress relaxation to occur. The tensile stresses appear to be limited to the softened weld zone resulting in a narrowing of the tensile region as the traverse speed increased.

Sutton et al [6] studied the microstructure of friction stir welds in 2024-T3 aluminum. Light microscope and scanning electron microscope (SEM) were used to capture the microstructure. In addition, energy dispersive X-ray spectroscopy (EDX) was used to analyze the chemical composition of the material. Microstructure as a function of transverse location and as a function of through-thickness location is shown in Figure 2-8. The results showed that more grain refinement occurred within the nugget, and that the grain size decreased as traveled from the top to the bottom and this is most likely due to higher heat input on the top causing additional grain growth. The results from metallurgical, hardness and quantitative EDX measurements showed that FSW can create a segregated banded microstructure consisting of alternating hard particle-rich and hard particle-poor regions.

Mahoney et al. [7] investigated the microstructure of friction stir processed NiAl Bronze alloy, they reported the initial microstructural evolution and resultant mechanical properties for the variety of the microstructures created by FSP which include Widmanstätten, equiaxed fine grain and banded or lamellar structure. The results reported by them showed that all the FSP microstructures have a significantly superior mechanical

properties compared to the as-cast microstructure. And the reasons for that are that FSP eliminate the casting defects as well as cause a significant refinement of the microstructure.

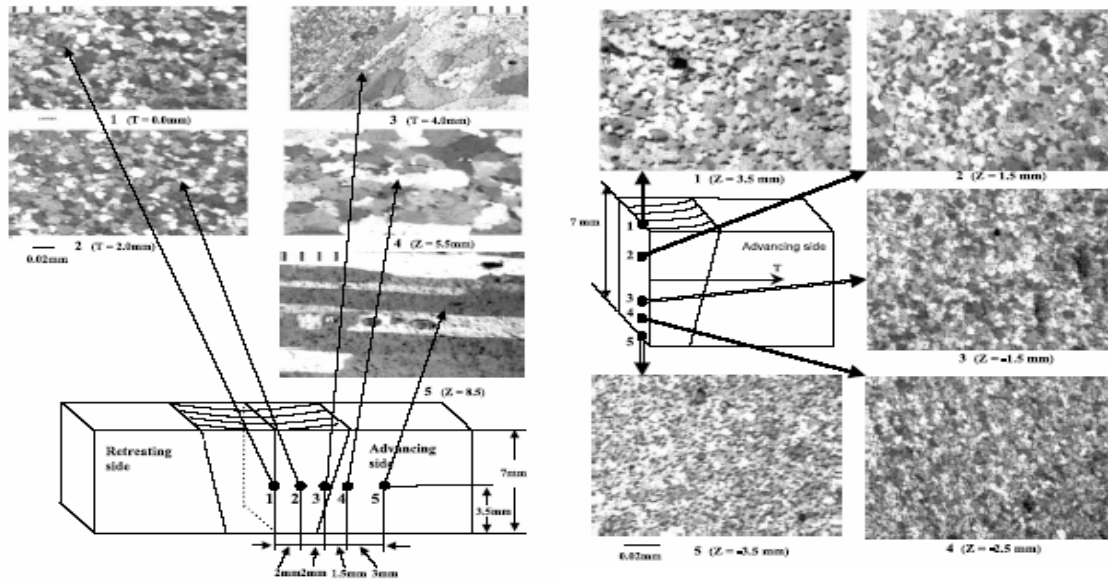


Figure 2- 7 Microstructure as a function of transverse and through- thickness locations [6]

Jata et al. [8] examined the microstructures of friction stir welds of Al-Li alloy using Optical and TEM microscopy to establish the mechanism of the evolution of microstructure in the dynamically recrystallized region of FSW welds. Using orientation imaging microscopy, many of the grain boundary misorientations created in the dynamically recrystallized region were observed to be between 15° to 35° . This suggested that the recrystallized grains in that region caused by continuous dynamic recrystallization mechanism. It was concluded that the grain size was found to have the same dependence on the Zener-Holloman parameter as material deformed via conventional hot working process for using reasonable estimates of the strain rate and temperature in the FSW nugget.

Bensavides et al. [9] investigated the microstructures of Al 2024 friction stir welds and compared the grain sizes of friction stir welding at room temperature (30°C) and at low temperature (-30°C). They observed that there was an increase in the weld

zone equiaxed grain size from the bottom to the top at room temperature but at low temperature there is a smaller difference from bottom to top. Furthermore, the grain size is considerably smaller in the low-temperature weld. These observations are consistent with the grain growth relations which states that there is a direct relation between temperature and grain growth. The average grain sizes obtained were measured to be between 3 and 0.65 μm .

Kwon et al. [10] investigated the hardness and tensile strength of the friction stir-processed 1050 aluminum alloy. They observed that the hardness and tensile strength increased significantly with decreased tool rotation speed as shown in Figure 2-9. The results showed that at 560 rpm, the hardness tensile strength increased as a result of grain refinement by up to 37% and 46% respectively compared to the as-received material. The hardness was higher on the advancing side than that of the retreating side. Kwon et al. concluded that the results demonstrate that the friction stir processing technique is highly effective for creating improved mechanical properties resulting from grain refinement.

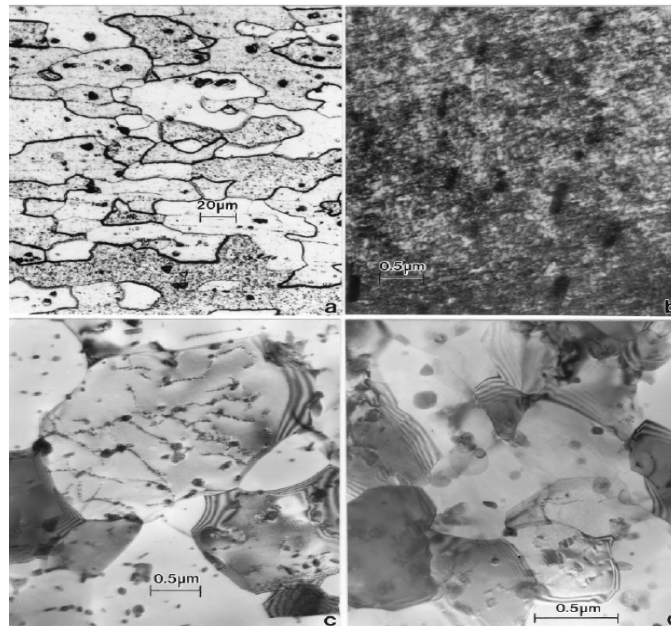


Figure 2- 8 Comparison of room temperature and low-temperature FSW microstructures in 2024 Al with the base metal microstructures. (a) Light metallographic view of base metal. (b) TEM view of base metal. (c) TEM view of room-temperature weld zone center. (d) TEM view of low-temperature weld zone center. Note dense dislocation density in (b) in contrast to (c) and (d) [10]

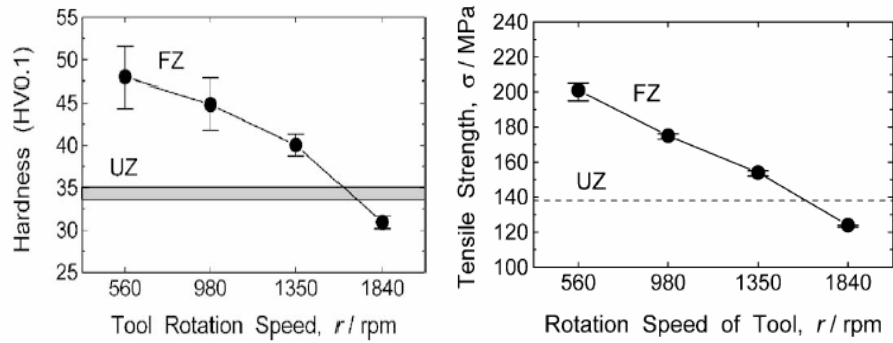


Figure 2- 9 Average hardness and tensile strength for unprocessed zone and friction stir zone at different tool rotational speed [10]

Itharaju et al. [11] investigated the microstructure at different combinations of rotational and translational speeds and tried to relate the resulting grain sizes to the generated forces in friction stir processed 5052 aluminum sheet. They observed that the resulting average grain size of the FS processed AA5052 sheet were between 1.5 and 3.5 μm depending on the process parameters, compared to 37.5 μm for the unprocessed sheet, which mean that great refinement has been achieved. Itharaju et al also concluded that, in general, the plunging force increases with increasing rotational speed and it is almost independent of the translational speed.

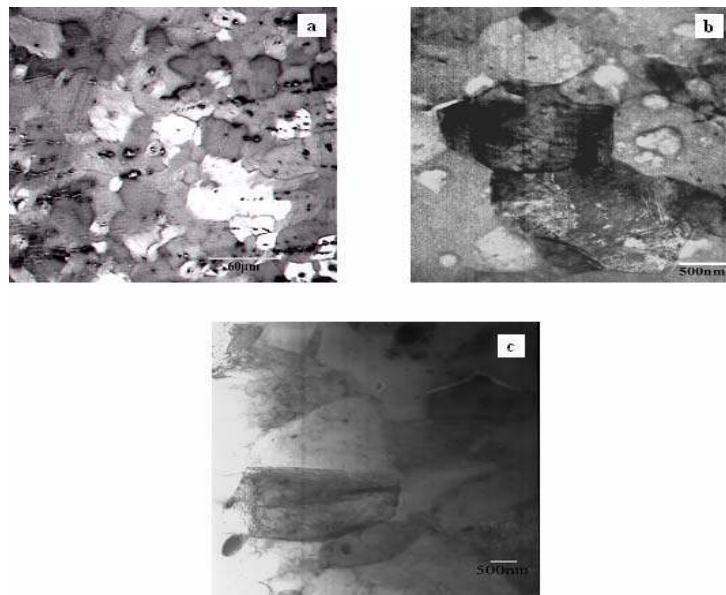


Figure 2- 10 Unprocessed AA5052 sheet (a, Optical Microscope), FS processed zone at 600rpm, 2.5in/min. (b, TEM), and FS processed zone at 800, 2.5in/min. (c, TEM). [11]

2.4-2 Superplasticity

Friction stir processing (FSP) is believed to have a great potential in the field of superplasticity. The fine and homogenous grain structure produced by FSP makes it gain this techniques impressive for the superplasticity researcher. Microstructural investigations, tensile tests at different temperature and different strain rates, and even superplastic forming of friction stir processed sheet were investigated.

Mishra et al [12] presented the effects of overlapping passes of friction stir processing on superplasticity in Aluminum alloys. 7075 Aluminum sheet were friction stir processed by nine overlapped passes. A constant velocity punch forming tests were conducted to investigate the effect of strain rate on forming. Also, tensile tests were performed for several samples taken from various areas of the FSP sheet. The microstructural investigation showed that after FSP the grain became finer and equiaxed as shown in Figure 2-12.

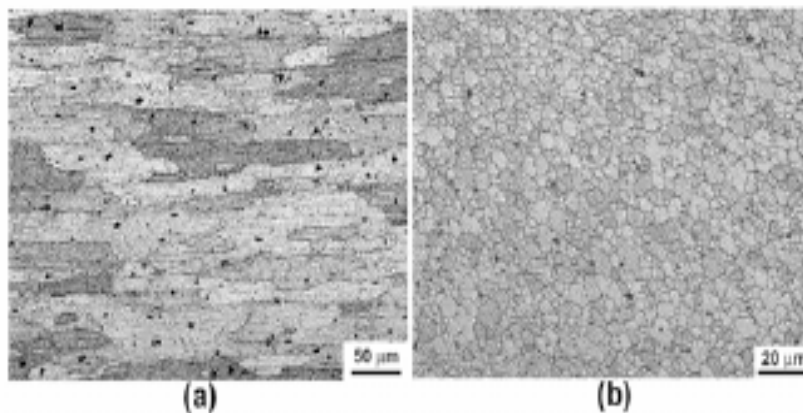


Figure 2- 11 Microstructure of 7075 Al alloy a) as received and b) FSP [12].

The tensile test results showed that the overlapped FSP exhibited superplastic behavior, but the as received sample did not exhibit superplastic behavior. Figure 2-13 shows the elongation versus temperature.

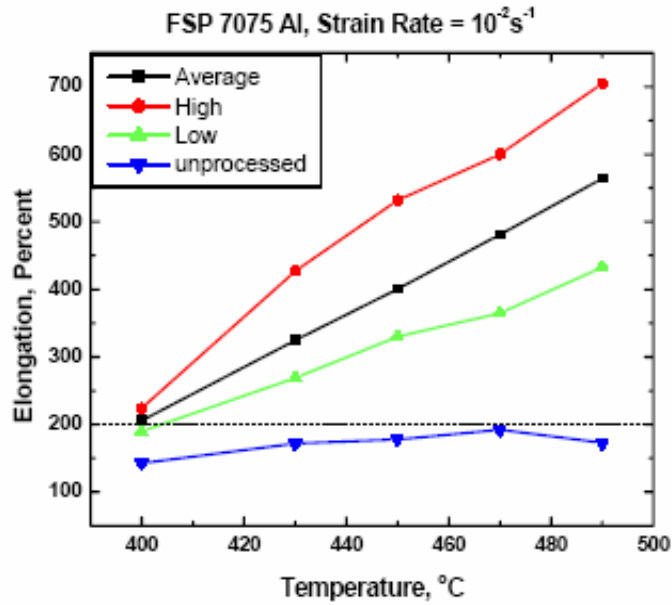


Figure 2- 12 Elongation versus temperature plots at initial strain rate of 10^{-2} s^{-1} for the nine pass FSP alloy [12].

Ma et al. [13] investigated the superplasticity in friction stir processed cast A356 at different temperature and strain rate. Single pass of friction stir processing was used, and optical microscope and TEM were used to investigate the microstructure. Tensile tests for mini tensile samples were also conducted. The stress strain behavior is shown in Figure 2-14 and comparison of elongation for both FSP and cast conditions as functions of temperature and strain rate are shown in figure 2-15.

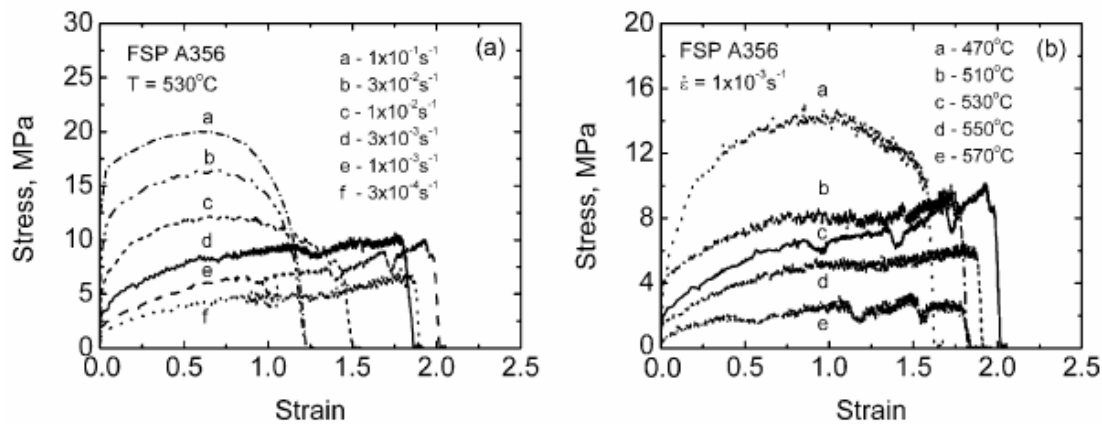


Figure 2- 13 Stress-strain behavior of FSP A356 as a function of a) initial strain rate at 530 °C and b) temperature at an initial strain rate of $1 \times 10^{-3} \text{ s}^{-1}$ [13].

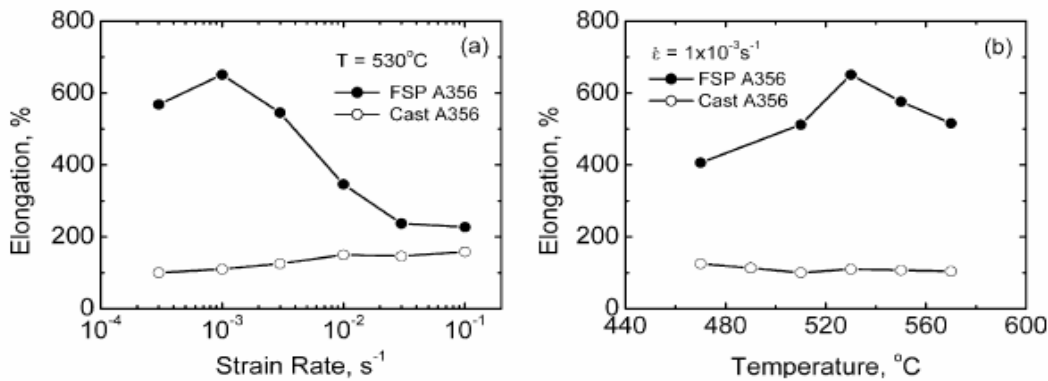


Figure 2- 14 Variation of elongation with a) initial strain rate and b) temperature for both FSP and cast A356 [13].

Ma et al concluded that FSP converted a non-superplastic cast A356 to superplastic with maximum elongation of 650% at 530 °C and initial strain rate of $1 \times 10^{-3} s^{-1}$. The flow stress of FSP A356 was also significantly lower than that of cast A356.

Salem et al. [14] investigated the ability of friction stir welded 2095 sheet to maintain superplastic behavior in the weld region. They stated that higher welding rates result in higher % elongation to fracture. A welding rate of 2.1 mm/s at 1000 RPM caused sub-grain coarsening that resulted in reduced superplastic capability. High welding rates increased the density of dislocations and develop microstructures consisting of tangled dislocation structures and sub-grains with small misorientations. Sheets welded at 3.2 and 4.2 mm/s displayed uniform superplastic deformation up to strains of ≈ 1.3 . At the cessation of uniform deformation, necking took place within the region adjacent to the friction stir weld nugget, followed by fracture.

Charit et al. [15] suggested that friction stir processing of commercial 2024 alloy can be used as a simple and effective technique to produce microstructure suitable for superplasticity at high strain rates and lower temperature and lower flow stress. The following observations were presented; abnormal grain growth throughout the weld nugget at SPF temperatures resulted in reduction of room temperature mechanical properties, however the microstructure in the weld HAZ is stable and retains superplastic properties. So the critical issue confronting the practical realization of FSW/SPF

technology for aluminum alloys was the thermal stability of the fine-grain microstructure in friction stir welded regions at SPF temperatures. Charit et al. concluded that superplasticity is achieved in 2024 alloy at higher strain rate and lower temperature via friction stir processing.

Ma et al. [16] investigated friction stir processing of commercial 7075Al rolled plates with different processing parameters. The microstructural investigation showed that FSP resulted fine-grained of 3.8 and 7.5 μm . They observed that heat treating the FS processed sheets at 490 °C for an hour showed that the fine grain microstructures were stable at high temperatures. Superplastic investigations in the temperature range of 420–530 °C and strain rate range of 1×10^{-3} – $1 \times 10^{-1} \text{ s}^{-1}$ were carried out and they demonstrated that a decrease in grain size resulted in significantly enhanced superplasticity and a shift to higher optimum strain rate and lower optimum deformation temperature. Ma et al. concluded that the mechanism which was responsible for the superplastic behavior of the FS processed 7075 Al was the grain boundary sliding.

Dutta et al. [17] performed a deep cup forming by superplastic punch stretching of multiple overlapping passes of friction stir processed 7075 Al alloy plate. Forming at different strain rates was done. Figure 2-16 shows three cups punch formed of as received and FSP plate at different strain rate. FEM simulation of the forming process was also done to predict the load and thickness variations, the simulation results showed good prediction of the load as well as the thickness variations up to the beginning of instability.

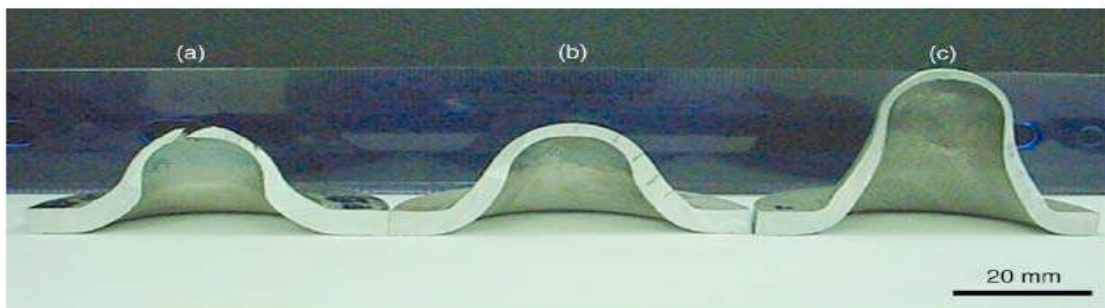


Figure 2- 15 Three cups punch formed at 723 K: (a) as-received; (b) FSP at 18.5mm punch stroke; (c) FSP at 28.5mm punch stroke. [17]

2.4-3 Modeling:

There is not much work that has been done in modeling friction stir processing. Most of the modeling work focus on thermal issues of the process. Other researchers proposed mechanical models that deal with stresses strain and generated forces. However limited work has been done to develop coupled thermo-mechanical models that combine mechanical and thermal aspects of the process. Other part of modeling work that been done is microstructural modeling. Again the there is very limited modeling work that combine mechanical, thermal and microstructural parts of the process.

Ulysse [18] proposed a 3-D visco-plastic modeling for friction stir welding; the main goal of this work was to determine the effect of tool speed on the temperature. In his mechanical model, Ulysse assumes a rigid visco-plastic material where the flow stress depends on the strain rate and temperature and can be represented by inverse sine-hyperbolic relation as follows:

$$\sigma = \frac{1}{\alpha} \sinh^{-1} \left[\left(\frac{Z}{A} \right)^{1/n} \right], \quad Z = \dot{\epsilon} \exp \left(\frac{Q}{RT} \right) \quad (2.1) [18]$$

Where α , Q , A , n are material constants, R the gas constant and T is absolute temperature. With the material constants determined by using standard compression tests and after applying the appropriate boundary conditions, the mechanical model is complete. Then he used the conductive convection steady-state equation to describe his thermal model.

$$\rho c_p u \nabla \theta = \nabla \cdot (k \nabla \theta) + \dot{Q} \quad (2.2) [18]$$

Where ρ is density, c_p the specific heat, u the velocity vector, k the conductivity, θ the temperature and \dot{Q} is internal heat generation rate. Ulysse assumes that the heat generation rate can be expressed as the product of the effective stress and the effective strain rate based on the assumption that about 90% of the plastic deformation is converted

into heat. Based on the thermal and mechanical models Ulysse developed a numerical model to predict the effect of tool speed and rotational speed on the temperature distribution within the plate. He validated his model by comparing predicted results with experimental data obtained by using thermocouples. In general the predicted temperature tends to be higher than that obtained experimentally. Figures 2-17 and 2-18 show some results of Ulysse work.

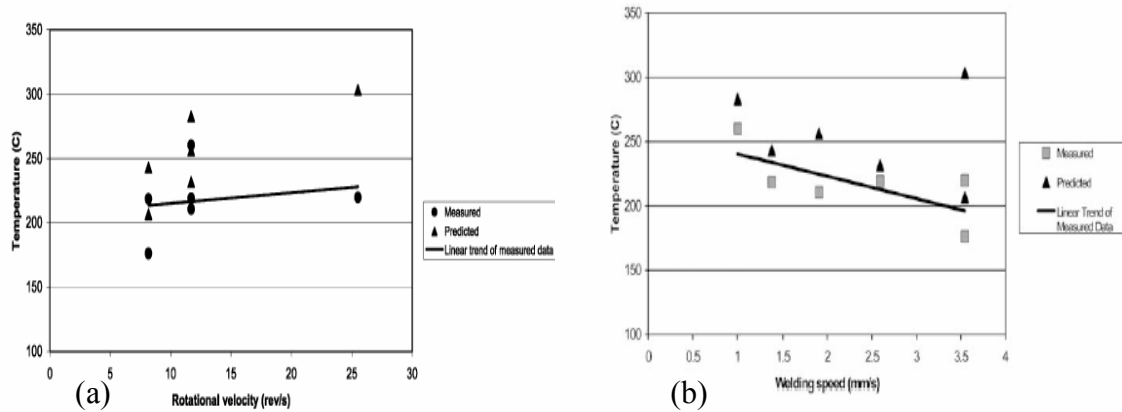


Figure 2- 16 Stir welding temperature as a function of (a) rotational speed and (b) welding speed [18]

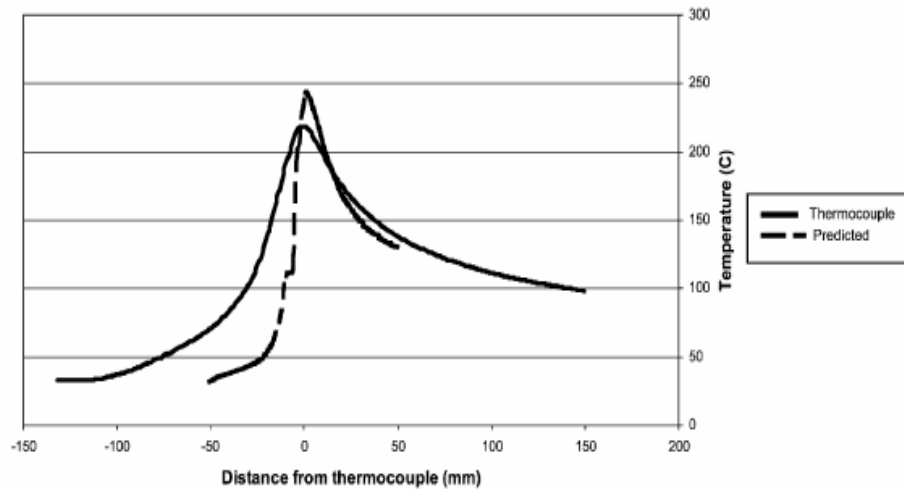


Figure 2- 17 Temperature profile at 8.2 re/s and 1.4 mm/s [18]

Chang et al. [19] proposed a relation between grain size and Zener-Holloman parameter during friction stir processing in AZ31 Mg alloys. It is shown that the working

temperature and the strain rate have a great influence on the resulting grain size in extruded Mg based alloy. So the Zener-Holloman parameter which is a function of strain rate, temperature and material constants appears to be appropriate to be related to the resulting grain size in friction stir processing.

$$Z = \dot{\varepsilon} \exp\left(\frac{Q}{RT}\right) \quad (2.3) [19]$$

Where $\dot{\varepsilon}$ is the strain rate, R is the gas constant, T is the temperature, and Q is the related activation energy. The material flow during FSP was driven by the rotating pin. The material flow (R_m) is related to the pin rotational speed (R_p), R_m may be equal or less than R_p according to the contact condition (sticking or sliding). A simple linear assumption has been made so the average $R_m=0.5 R_p$. So the torsion type deformation that occurs during FSP the material flow strain rate can be expressed as:

$$\dot{\varepsilon} = \frac{R_m \cdot 2\pi r_e}{L_e} \quad (2.4) [19]$$

Where r_e and L_e are the effective (average) radius and depth of the dynamically recrystallized zone. The temperatures data used were obtained experimentally and the grain sizes were obtained by microstructural characterization using optical microscopy and scanning electron microscopy (SEM). Using these results which are shown in Figure 2-19, a relation between grain size diameter (d) and Zener-Holloman parameter (Z) during friction stir processing in AZ31 Mg alloys is quantitatively given by Chang et al:

$$\ln d = 9.0 - 0.27 \ln Z \quad (2.5) [19]$$

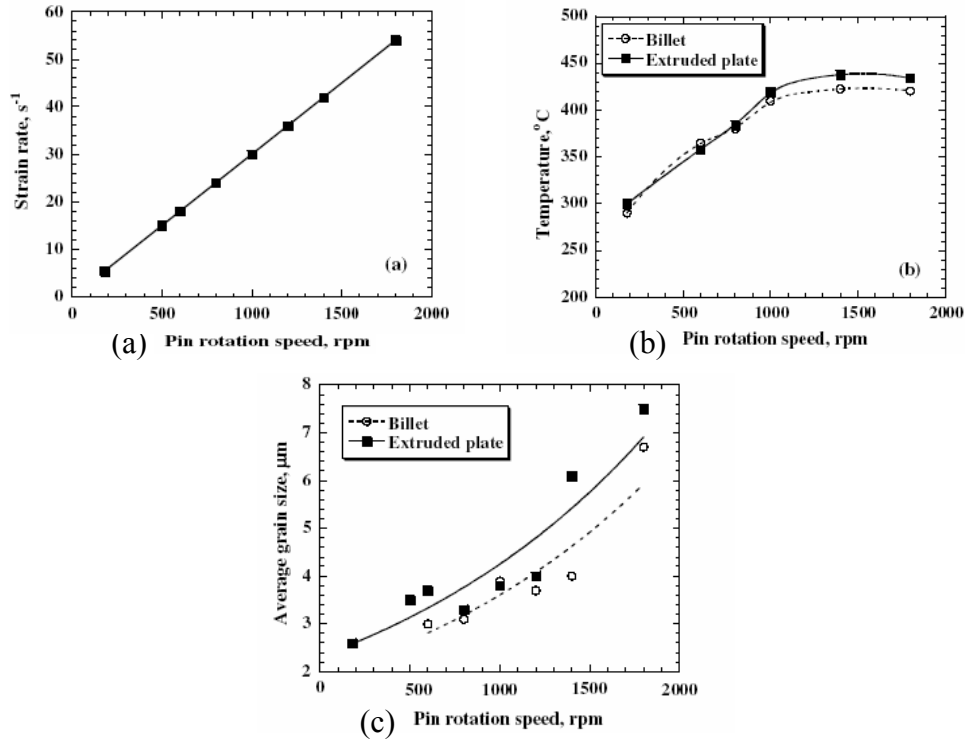


Figure 2- 18 Variations of the (a) strain rate (b) temperature and (c) the average grain size as a function of pin rotation speed [19]

Heurtier et al. [20] proposed a thermomechanical analysis of the friction stir welding process. A model of material flow pattern is proposed in this work; two zones within the weld are considered, the flow is assumed to be incompressible and kinematically admissible, using classical fluid mechanics the velocity fields in these zones were developed. The welding zone is divided into two parts; the first zone is located just below the shoulder of the tool. In this zone the bulk material flowing around the screw head pin (translation velocity field) is submitted to an additional torsion velocity field. This torsion is imposed by friction of rotating shoulder on surface and partially affects the depth of the metal sheets over a range of 1 or 2 mm. The second zone is located within the depth of the welded zone (nugget zone and thermomechanically affected zone). It is submitted to the translation motion of the pin and the vertical motion of the bulk material, dragged down by the screwing kinematics of the tool. The velocity fields within the two zones are shown in equations 2.6 and 2.7.

First zone:

$$\begin{aligned}
 u &= V \left[1 - a^2 \frac{x^2 - y^2}{(x^2 + y^2)^2} \right] - y V_{tor} \frac{z}{L} \\
 v &= V \left[-\frac{2xya^2}{(x^2 + y^2)^2} \right] + x V_{tor} \frac{z}{L} \\
 w &= 0
 \end{aligned} \tag{2.6} [20]$$

Second zone:

$$\begin{aligned}
 u &= V \left[1 - a^2 \frac{x^2 - y^2}{(x^2 + y^2)^2} \right] + \frac{kz}{T^2 + z^2} (\cos \Phi) \frac{1}{\sqrt{x^2 + y^2}} \\
 v &= V \left[-\frac{2xya^2}{(x^2 + y^2)^2} \right] + \frac{kz}{T^2 + z^2} (\cos \Phi) \frac{1}{\sqrt{x^2 + y^2}} \\
 w &= -\frac{kT}{T^2 + z^2} \frac{1}{\sqrt{x^2 + y^2}}
 \end{aligned} \tag{2.7} [20]$$

Where V_{tor} is the parameter for the torsional velocity, z the height, L the length of the first zone, V the translation velocity of the tool, a the screw radius, and k and Φ identify the vortex velocity. In this work the velocity fields are function of the torsional velocity of the material itself, which linearly extrapolate of the rotation velocity of the tool. From the velocity fields obtained, it is possible to find the strain path of the material within the weld. Also the temperature within the weld was predicted with the assumption that the whole plastic power is dissipated into heat then. Heurtier et al presented predicted strain map results and predicted temperature distribution.

Schmidt et al. [21] proposed an analytical model for the heat generation in friction stir welding, different contact conditions between the tool and the weld are studied; sliding, sticking and partial sliding/sticking . Also experimental results for plunge force and torque are also presented to determine the contact condition. Schmidt defined the three contact states; sticking condition: where the material of weld stick to the tool surface, and this happens when the friction shear stress exceeds the yield shear stress of

the weld and so the material of weld have the tool velocity, sliding condition: which occurs when the contact shear stress is smaller the yield shear stress of the weld here the weld segment shears slightly to a stationary elastic deformation, where the shear stress equals the dynamic contact shear stress, partial sliding/sticking which is a state between sliding and sticking. And to identify the contact condition Schmidt proposed a contact state variable δ which is defied as:

$$\delta = \frac{v_{matrix}}{v_{tool}} = 1 - \frac{\dot{\gamma}}{v_{tool}} \quad (2.8) [21]$$

$$\dot{\gamma} = v_{tool} - v_{matrix}$$

Where $\dot{\gamma}$ is the slip rate, so when δ is 1 then it is the sticking condition, for δ is 0 then it is sliding condition and when $0 < \delta < 1$ then it is partial sliding/sticking condition.

Stewart et al. [22] proposed a combined experimental and analytical modeling approach to understanding friction stir welding. Stewart presented two models for friction stir welding process, the Mixed Zone and the Single Slip Surface model and compared their predictions to experimental data.

In the Mixed Zone model the rotational slip of the material assumed to take place within the whole plastic zone and not only on the tool-workpiece interface, the velocity within the plastic zone flows in vortex pattern to match the angular velocity of the tool at the tool-workpiece interface and drooped to zero at the edge of the plastic zone, in this model a finite region of continues gradients of deformation material surrounding the pin tool. By using simple stress temperature relation the results was inadequate to predict the weld characteristics, but after considering the effect of the strain rate the predictions were more realistic but still not matching the experimental observations.

For the Single Slip Surface model, the rotation slip assumed to take place a contracted slip surface outside the tool-workpiece interface, the results of this model showed a good agreement with the experimental measurements of thermal field, forces and shape of the weld region. But this model did not account for the three dimensional effects.

Arbegast [23] proposed a simple model based on metalworking process. Arbegast in his work attempted to develop relationships for calculating width of extrusion zone, strain rate and pressure. Also he showed empirical relations between process parameters, maximum temperature and material constitutive properties. As the pin moves forward the material is heated and the state of stress exceeds the critical flow stress and so the material flows; the material is forced upwards into the shoulder zone and downwards into the extrusion zone, and a small amount of material is captured beneath the pin tip where a vortex flow is exists (this zone is called swirl zone). Also there is a forging zone where the material from the front of the pin is forced under a hydrostatic pressure conditions into the cavity left by the forward moving pin tool. Metal flow patterns proposed by Arbegast are shown in Figure 2-20.

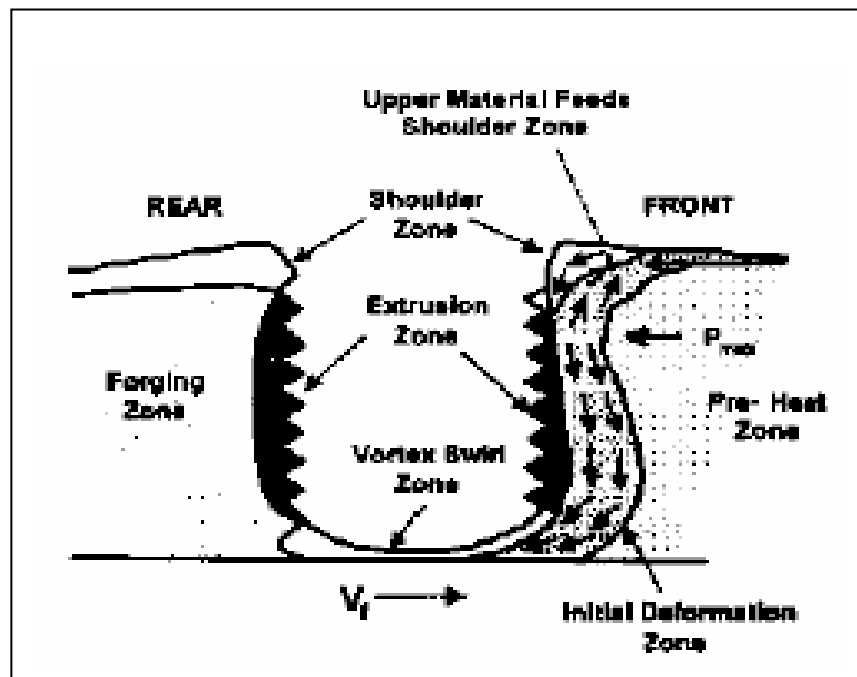


Figure 2- 19 Metal flow patterns during friction stir joining [23]

Arbegast use an empirically determined constitutive equation to determine the flow stress as a function of strain rate and temperature as shown in equation 2.9.

$$\begin{aligned}
\sigma_{0.1} &= \exp(b) \exp(mT) \\
m &= m_1 \dot{\epsilon}^2 + m_2 \dot{\epsilon} + m_3 \\
b &= b_1 \dot{\epsilon}^2 + b_2 \dot{\epsilon} + b_3
\end{aligned}
\tag{2.9} [23]$$

Where $\sigma_{0.1}$ is critical Gleeble flow stress, b is the strain rate exponent and m is temperature compensated strain rate exponent b, m were determined for each alloy through a series of curve fittings.

Arbegast use a simple thermal model to predict the maximum temperature, it was observed that the maximum temperature was a strong function of rotational speed, and the heating was a strong function of forward speed also it was noted that there was a slightly higher temperature on the advancing side, the thermal model presented by Arbegast is shown in equation 2.10.

$$\frac{T}{T_m} = K \left(\frac{\omega^2}{v_f \cdot 10^4} \right)^a
\tag{2.10} [23]$$

Where T_m is the melting point temp., ω is the rotational speed and v_f is the forward velocity, a is found to be between 0.4-0.6 and K is between 0.65-0.75.

The main assumptions made by Arbegast to develop the metal flow model are; The process can be modeled after a simple extrusion process and the temperature and strain rate dependence of the flow stress is not included (this means the model is material independent).

Arbegast presented constitutive relation for the flow stress as a function of strain rate and processing temperature, also a simple thermal model is presented to predict the maximum temperature, the optimum width and strain rate is also determined, also the extrusion pressure was also approximated as a function of material, tool pin geometry and process parameters . But still three dimensional temperature profile and extrusion zone are needed. Also using finite element method to calculate the states of stresses at all points will be helpful.

Schneider et al [24] proposed mathematical model to describe the material flow path in friction stir welds. They suggested that there are three incompressible flow fields that together describe the material flow in friction stir welds. Figure 2-21 shows the flow fields in friction stir welds. The first field is a rigid-body rotation which is identical to the rotation of the tool spindle and bounded by a cylindrical shear surface. The second field is a homogenous and isotropic velocity field with the velocity equal and opposite to the travel velocity of weld-tool. The third is a ring vortex flow in which the metal moves up and down.

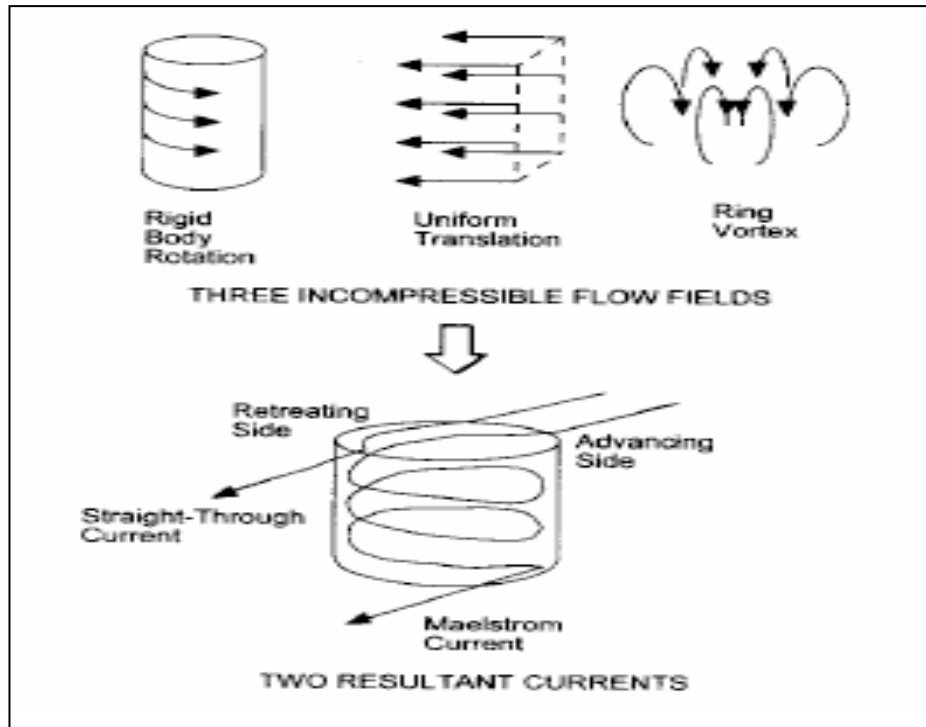


Figure 2- 20 Material flow fields in friction stir welds [24]

To investigate the material flow, Schneider inserted thin tungsten wire inside the FSW seam; if the shear stresses are severe then the wire will break, as a result of tension if the wire is flexible and as a result of bending if the wire is stiff. Experimental results showed that the wire was broken into uniform segments; the broken segments showed a slight necking at the edges this observation support that a tensile failure mode is occurred. Most of the wire segments are arrayed in a straight line this suggests that a rigid body rotation

at the tool superposed by uniform translation would exhibit the same flow pattern of streamlines in the plane view.

Reynolds et al. [25] discussed two models of the friction stir welding process; input torque based thermal simulation, and 2-D fluid dynamics based model. In the input torque based thermal model the average shear stress at the workpiece/tool interface is assumed, and then the heat input is correlated to the measured torque. Reynolds divided the total torque into three parts:

$$1) \text{ Torque at the shoulder interface: } M_{\text{shoulder}} = \int_{r_i}^{r_o} (\tau r)(2\pi r) dr \quad (2.11) [25]$$

$$2) \text{ Torque at the pin bottom: } M_{\text{pinBottom}} = \int_0^{r_i} (\tau r)(2\pi r) dr \quad (2.12) [25]$$

$$3) \text{ Torque at the vertical pin surface: } M_{\text{pinSurface}} = (\tau r_i)2\pi r_i h \quad (2.13) [25]$$

Where r_i , r_o are pin and shoulder radiuses, τ is the average shear stress (flow stress) and h is the pin height. Then the total torque is related to the average power (P_{av}) input and hence the total heat input (Q_{tot}).

$$M_{tot}\omega = P_{av} = \dot{Q}_{tot} \quad (2.14) [25]$$

The output of this model was a time/temperature history which can be used to rationalize observed differences in weld properties and microstructure.

In the 2-D fluid dynamics based model, flow past a rotating cylinder with a no slip boundary condition at the tool workpiece interface, the effective deviatoric stress expressed as a function of temperature and strain rate as shown in equation 2.15. The dynamic viscosity is temperature and strain rate dependent calculated using Prezna's viscoplasticity model as shown in equation 2.16.

$$\sigma(T, \dot{\varepsilon}) = \frac{1}{\alpha} \ln \left\{ \left[\frac{Z}{A} \right]^{1/n} + \left(\left[\frac{Z}{A} \right]^{2/n} + 1 \right)^{1/2} \right\} \quad (2.15) [25]$$

$$\eta(T, \bar{\dot{\varepsilon}}) = \frac{\sigma(T, \bar{\dot{\varepsilon}})}{3\bar{\dot{\varepsilon}}} \quad (2.16) [25]$$

Where Z is the Zener-Holloman parameter, $\bar{\dot{\varepsilon}}$ is the effective strain rate, T is the temperature, Q and R are constants, and α , n and A are constants determined by fitting to experimental data. The main limitations of using this viscosity formulation are; the lack of a strain history effect on the flowing material (no strain hardening), and the neglect of elastic deformation.

Fratini et al. [26] proposed a numerical model that aimed to the determination of the average grain size due to continuous dynamic recrystallization phenomena in friction stir welding of AA6082 T6 aluminum alloy. The proposed model takes into account the local effects of strain, strain rate and temperature on the average grain size. The final size of the continuously recrystallized grain is influenced by the local value of few field variables, such as the strain, the strain rate and the temperature levels as well as the considered material. They implement the model shown in equation 2.17 for the grain size evolution.

$$D_{CDRX} = C_1 \varepsilon^k \dot{\varepsilon}^j D_0^h \exp\left(-\frac{Q}{RT}\right) \quad (2.17) [26]$$

Where D_{CDRX} is the average grain size due to continuous dynamic recrystallization, ε is the equivalent strain, $\dot{\varepsilon}$ is the strain rate, D_0 is the initial grain size, Q is the continuous dynamic recrystallization activation energy, R is the universal gas constant, T is the absolute temperature and C_1, k, j and h are material constants. Good agreement with experimental results was obtained as shown in Figure 2-22.

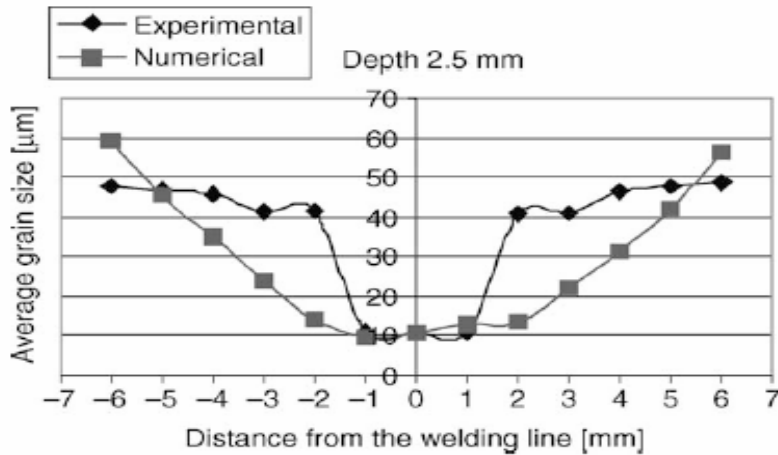


Figure 2- 21 Comparison between the measured and the calculated average grain sizes (FEW6-715 rpm, 71.5 mm/min, and depth 2.5 mm) [26]

Chen et al. [27] proposed a three-dimensional model based on finite element analysis to study the thermal history and thermo-mechanical process in the butt-welding of aluminum alloy 6061-T6. The model incorporated the mechanical reaction of the tool and thermo-mechanical process of the welded material. The heat source incorporated in the model involves the friction between the material and the probe and the shoulder. In this model the tool was assumed to be rigid solid, and the material is ductile with elasticity, plasticity and kinetic hardening effects. The X-ray diffraction (XRD) technique is used to measure the residual stresses in the welded plate. It was observed that the maximum temperature gradients in longitudinal and lateral directions are located just beyond the shoulder edge; also the residual stress was greater in the longitudinal direction than that of the lateral.

Song et al. [28] presented a three-dimensional heat transfer model for FSW. The heat generated by the tool pin and shoulder were considered in this work, and were assumed to be frictional heat. A moving coordinate was also used to reduce the difficulty of modeling a moving tool. Finite different method was used to solve the control equations. Thermocouples and infrared camera were used to measure the temperature histories in order to verify the presented model. Song et al concluded that coupled heat-transfer process for both the tool and workpiece during FSW can be easily applied

because of the use of moving coordinate instead of moving heat source. Song et al suggested that preheating is beneficial to increase the temperature in the front of the tool, and this makes the material easily be welded and protect the tool from being worn out.

Dong et al. [29] presented coupled thermomechanical analysis of FSW process using simplified models. Three numerical models were introduced; coupled friction heat generation, plastic flow slip zone development and three-dimensional heat and material flow. The coupled thermomechanical friction heating is predominant in the upper region and plastic work induced heating predominant in the lower region, they suggested that both heat mechanisms have to be considered. Dong et al. observed that pin geometry and workpiece thickness are the critical parameters that affect the formation of the slip zone, and also that the material flow can be characterized as a boundary layer flow phenomenon.

Askari et al. [30] presented three-dimensional analysis to capture the coupling between tool geometry, heat generation and plastic flow of the material. The model solved; the steady-state continuity and momentum balance equations and the steady-state energy equation. Askari et al. predicted the temperature, flow stress, vertical velocity and the plastic strain rate. The model was validated by experimental results obtained by thermocouples and marking experiments.

Xu et al. [31] focused in their work on the characterization of the material flow around the rotating tool pin by using finite element simulations. The simulation results were compared with the experimental observations. The FSW was modeled as two-dimensional steady-state problem, and the interface between the pin and the plates was modeled using two methods; slipping interface model and frictional contact model. The predictions of the material flow pattern using the two interface models were very similar, which suggested that it is much simpler to use slipping interface model in FSW simulation. The predicted results showed a good agreement with the experimental tracing, and it was observed that the material particles directly ahead of the rotating pin will travel behind the pin only from the trailing side of the pin.

Chen et al. [32] presented a three-dimensional model based on finite element method to study the thermal history in FSW, stress distribution and the mechanical forces. The comparison of simulated and the measured results for both the temperature and force showed a reasonable agreement. The results showed that the vertical force decreases with increasing the rotational speed and increases slightly with increasing the traverse speed, and the lateral force has a weak link to the rotational speed increases slightly with increasing the traverse speed.

CHAPTER-3 EXPERIMENTAL INVESTIGATION

The experimental work that has been done includes; investigation of the effects of process parameter (rotational and translational speeds) on the resulting microstructure, hardness and quality of the FS processed pass of AA5052 sheet. In this chapter, the material that been processed as well as experimental setup and procedures have been discussed. Grain structure and void analysis have been also discussed. The effects of rotational speed, translational speed, and position within the processed area on hardness are presented in this chapter.

3.1 Material

The material that was used in this work is commercial 5052 Aluminum alloy sheet with nominal thickness of 1/8” and the samples dimensions are 4x1 inches. The nominal compositions of the material is shown in Table 3-1.

Table 3- 1 Compositions of Aluminum Alloy 5052 (wt %) [34]

Si	Fe	Cu	Mn	Mg	Cr	Zn	Al
0.11	0.25	0.17	0.03	2.2	0.25	0.02	Balance

3.2 Experimental setup

One of the most important features of FSP is the utilization of readily available machines such as a milling machine, and using a simple inexpensive tool simple to conduct the process. In this section; the experimental setup and the basic equipment required to conduct FSP process are discussed.

FSP tool is very important and critical element of the process. The tool assembly which is shown in Figure 3-1 consists of a shoulder and concentric pin. The tools which are used in this work are made of H13 tool steel. Different tool configurations were used;

shoulder diameter of $\frac{1}{2}$ " and $\frac{3}{4}$ ", and shoulder with and without concavity are used. The pin diameter is $\frac{1}{4}$ " and the height of it is slightly shorter than the thickness of the sheet which is $\frac{1}{8}$ ". Threaded and non-threaded pin are used. Figure 3-1 shows the different FSP tool configurations that were used.

One of the important things that made FSP more convenient is that a readily available machine can be used to conduct the process. In this work HAAS VF-0F CNC vertical milling machine (shown in Figure 3-3) was used. Also a backing plate made of steel is used to support the samples, Figure 3-2 shows the backing plate which been used. The experimental setup that been used is illustrated in Figure 3-4.



Figure 3- 1 Different tool configurations



Figure 3- 2 Assembly of backing plate holding plates and sample



Figure 3- 3 HAAS VF-0F CNC vertical milling machine

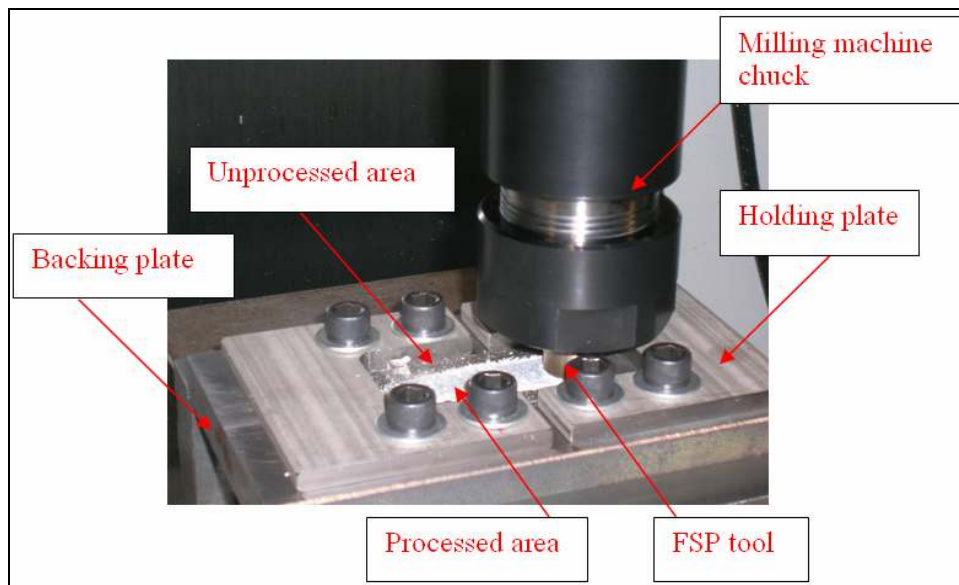


Figure 3- 4 Experimental setup

3.2-1 Experimental procedure

The sample that need to be friction stir processed have to be clamped firmly before the processing starts, so especially designed grooved baking plate and holding plates are used to hold the workpiece and keep it fixed during the processing . Then a small hole with same diameter as pin is drilled, instead of using the pin of the tool to start

penetrating the workpiece, this drilled hole avoid too much load on the tool for penetrating. Then the pin of the FSP tool is forced into the workpiece while it is rotating at the desired rotational speed, and the shoulder become in contact with the surface of the workpiece. The rotating FSP tool is then transverse along the desired direction with specific translational speed.

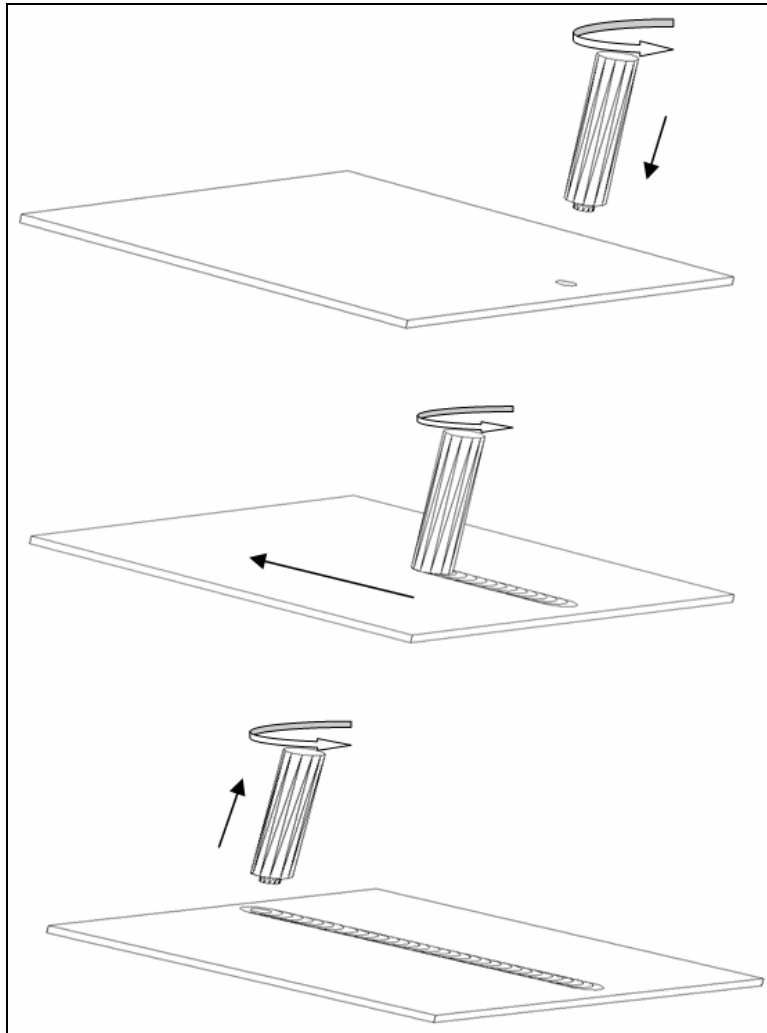


Figure 3- 5 Schematics of the stages of friction stir processing (FSP)

Frictional heating is produced from the rubbing of the rotating shoulder with the workpiece, while the rotating pin deforms and stirs the locally heated material. FSP is considered to be a hot working process where severe plastic deformation occurs within

the FS processed sheet. FS processed zone is characterized by dynamic recrystallization which results in grain refinement, and homogenous, equiaxed grain structure.

3.2-2 Microstructural investigation

The microstructural investigations are done in collaboration with the Department of Mechanical Engineering, Florida State University (FAMU-FSU). Various microscopy techniques were used to investigate the microstructure of a material. The main techniques used are: Optical microscopy, Scanning Electron Microscopy (SEM) which was used to give topographic information, and Orientation Imaging Microscopy (OIM) which was used to give more quantitative information. The sample preparation for the microscopic investigation includes grinding, diamond polishing and electro polishing. All microstructural samples were taken from the transverse section of the processed area at the middle of the sheet thickness as shown in Figure 3-6.

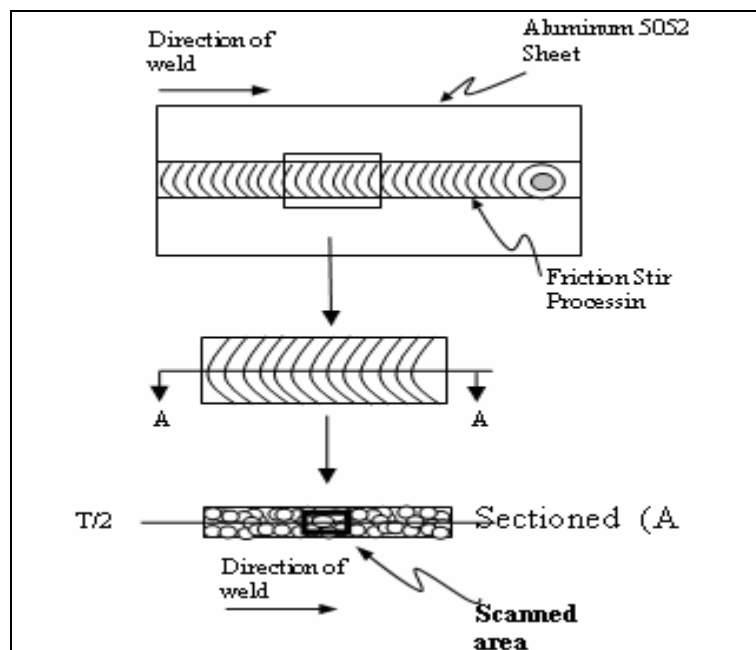


Figure 3- 6 Schematic of the prepared samples

Several samples with different combinations of rotational and translational speeds were investigated microscopically. Table 3-2 shows the processed samples at different combinations of rotational and translational speeds which were investigated.

Table 3- 2 Samples FS processed at different process parameters

Sample No.	Rotational Speed (rpm)	Translational speed (in/min.)
1	600	2.0
2	600	2.5
3	800	2.0
4	800	2.5
5	1000	2.0
6	1000	2.5

3.2-2 Hardness testing

Vickers Hardness of friction stir processed AA5052 samples were measured using Vickers hardness tester. The test load applied was 200 gf and the dwell time was 5 seconds. Various samples FS processed at different rotational and translational speed were tested and also different longitudinal positions were also tested. The averages of five values of hardness within each tested area were considered. All samples were taken from the transverse section of the processed area at the middle of the sheet thickness; the same as the samples for microstructural investigation (see Figure 3-6).

3.3 Results

In this section different results that show the effect of FSP on resulting microstructure are presented. Hardness results at different process parameters are also presented here. And the effects of the process parameters on the FSP pass quality.

3.3-1 Grain structure

The microstructural results using Orientation Imaging Microscopy (OIM) show the difference in grain size and homogeneity. As shown in Figure 3-7 the deformation zone consists of three zones: the nugget, the thermomechanical zone (TMZ), and the heat affected zone (HAZ). The grain size distributions are shown, and it is obvious that grain size within the nugget region is much smaller than other regions. Also it is observed that the heat affected zone is larger for the sample processed at 800 rpm than that processed at 600 rpm and this is because of the higher rotational speed which means more heat generated by friction.

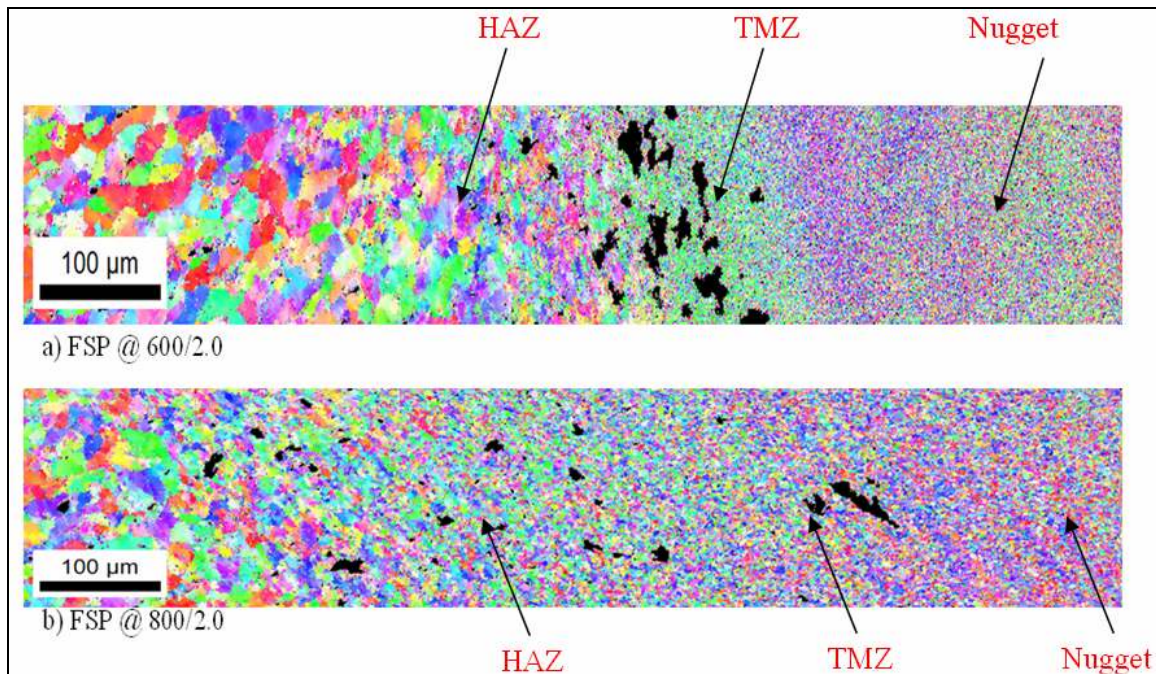


Figure 3- 7 The grain structure at different locations of the FS processed AA5052 sheet, at different conditions using OIM. (In collaboration with Department of Mechanical Engineering, FAMU-FSU)

Different samples were taken at the middle of nugget region and inspected using OIM. The results show that great grain refinements are achieved. The OIM map for the as received sample shows average grain size of 13.41 μm ; the average grain size is reduced to about 1.67 μm when FS processed at 600 rpm and 2.5 in/min. and to 4.49 μm when FS processed at 1000 rpm and 2.5 in/min. Figure 3-7 shows the OIM maps for as received sample and for different samples processed at different combinations of rotational and translational speeds. The average grain sizes for investigated sample are shown in Figure 3-8. It is observed that in general smaller grain size is obtained at lower rotational speed and at lower translational speed. This may be explained by the fact that as the rotational and translational speed increases more frictional heat is generated and so it is expected that the grain growth as a result of higher temperature is more dominant than the mechanical deformation. Another important observation is that FSP make the resulting grain structure more homogenous, and this is obviously shown in Figure 3-9.

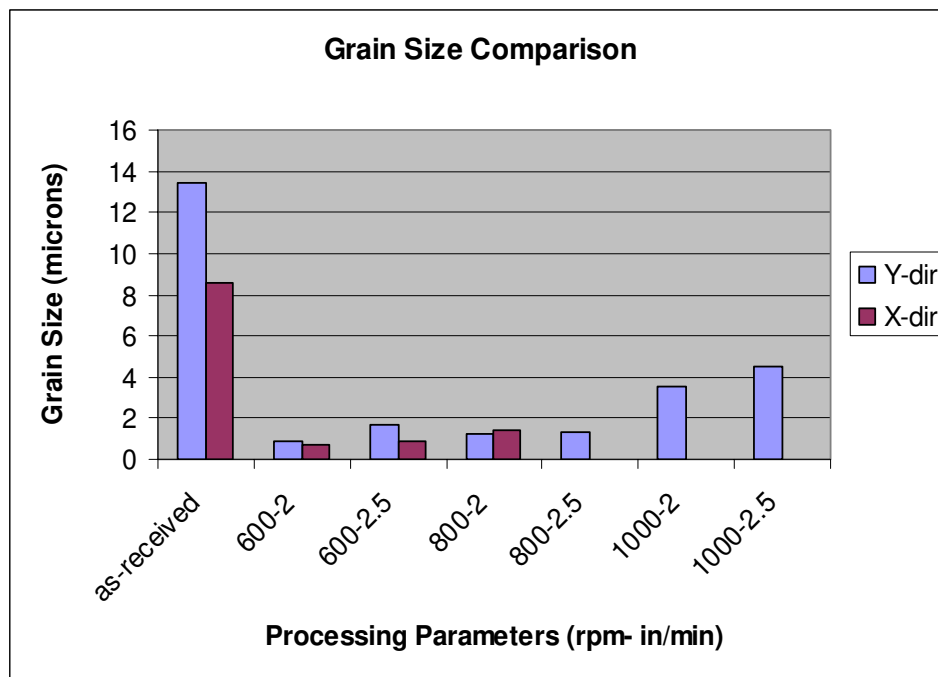


Figure 3- 8 Average grain size comparison of as received sample and FS processed at different process parameters combinations. *(In collaboration with Department of Mechanical Engineering, FAMU-FSU)*

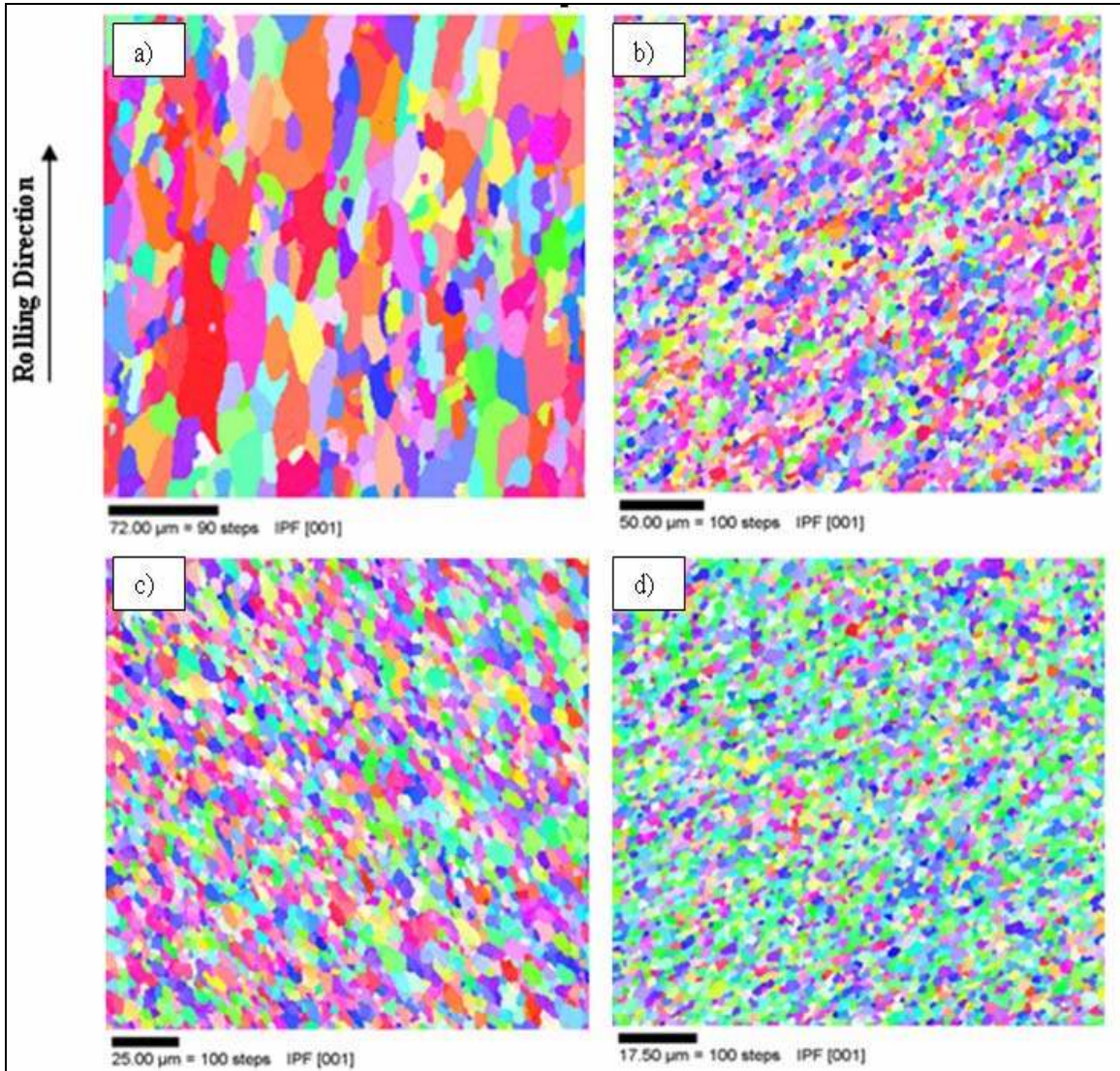


Figure 3- 9 The Orientation Imaging Microscopy Map of (a) As received AA5052 sample, (b) FSP at 1000 rpm and 2.5 in/min (sample B2), (c) FSP at 1000 rpm and 2.0 in/min (sample A2) and (d) FSP at 600 rpm and 2.5 in/min (sample B1) (*In collaboration with Department of Mechanical Engineering, FAMU-FSU*)

Figure 3-10 shows the misorientation angles for the as-received and for sample processed at 600 rpm and 2.5 in/min. It can be seen that though the median of the misorientation hovers around 49° , the entire profile is shifted towards the right. This is indicative of differential plastic deformation in adjacent grains [35].

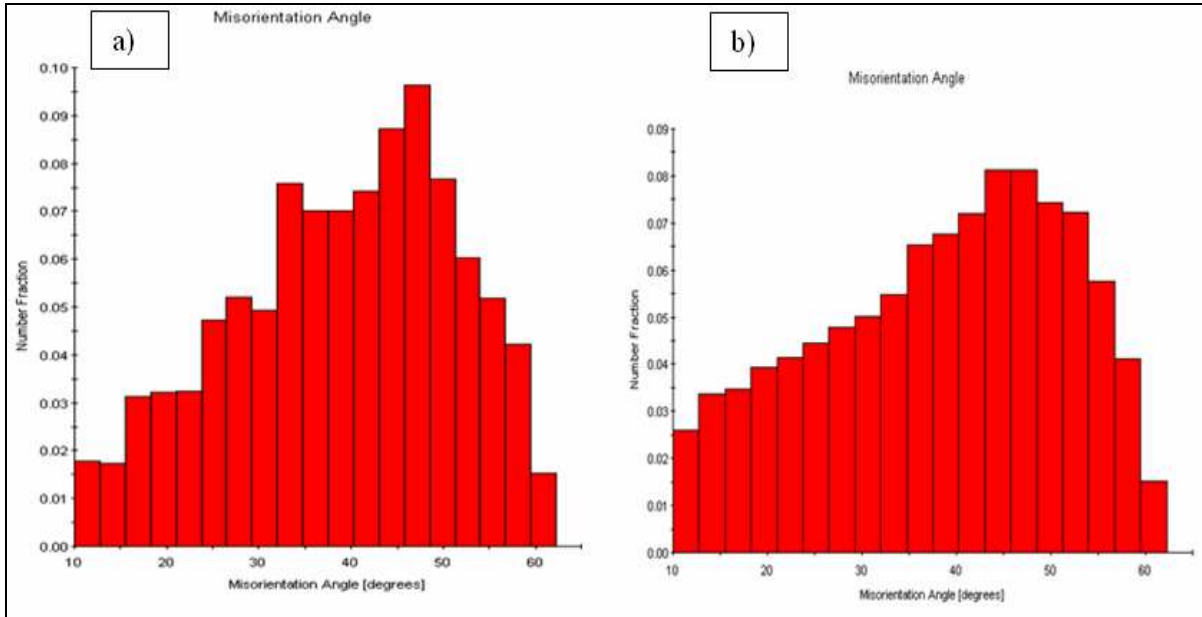


Figure 3- 10 The Average Grain Misorientation for; (a) as received sample, (b) FSP at 600 rpm and 2.5 in/min (sample B1) (*In collaboration with Department of Mechanical Engineering, FAMU-FSU*)

3.3-2 Hardness

The results show that the friction stir processed area has a higher Vickers hardness value than the original material. The effect of rotational speed on the resulting hardness is shown in Figure 3-11, and it is shown that as the rotational speed decreases the hardness increases and this agrees with the results reported by Sato et al. [36]. According to the Hall-Petch relationship the hardness increases as the grain size decreases, the hardness results supported the conclusion that more grain refinement is obtained at lower rotational speed. The effect of translational speed on the hardness was also investigated and the results which shown in Figure 3-12 show that, generally, as the translational speed increases the hardness increases.

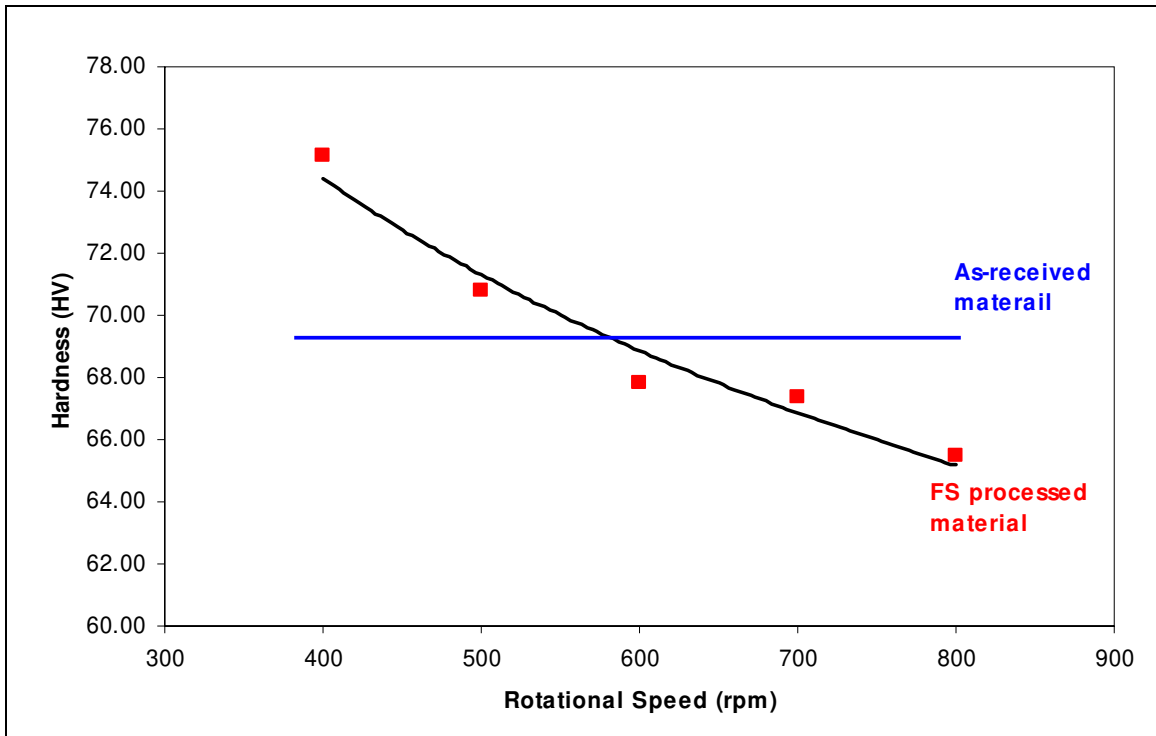


Figure 3- 11 Average hardness (HV) of FS processed at different rotational speed (translational speed is 2.0 in/min.)

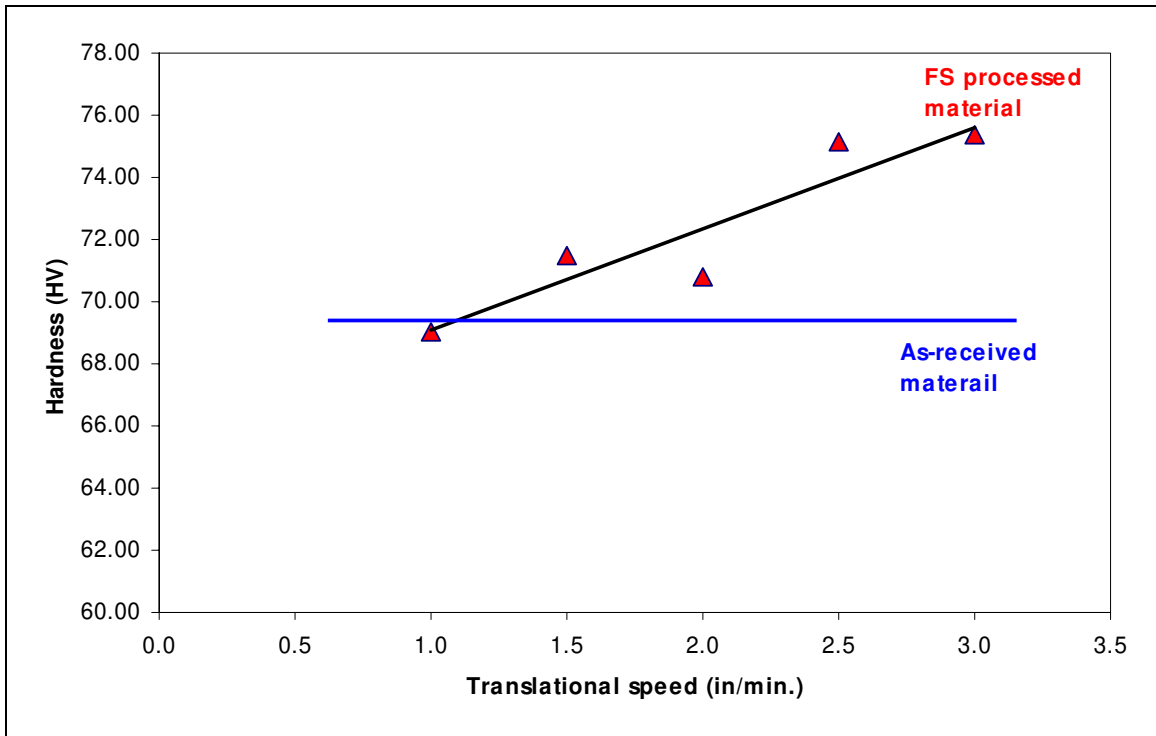


Figure 3- 12 Average hardness (HV) of FS processed at different translational speed (rotational speed is 500 rpm)

The hardness varied at different longitudinal positions of the processed area. This variation is believed to be caused by the variation of the temperature reached at different positions. Figure 3-13 shows that the hardness values are higher at the beginning of the FSP pass and decreases as going farther. Again the hardness decreases as going from top to the bottom (see Figure 3-14), and this variation might be explained by the variation of the temperature reached at different depths and the amount of deformation (see CH. 4). Generally the hardness of the FS processed area has a direct relation with temperature reached in that area. As the temperature increases the hardness decreases and this might be explained by the fact that more grain growth is taking place at higher temperature. Therefore larger grain sizes are produced according to the Hall-Petch relation at lower hardness values.

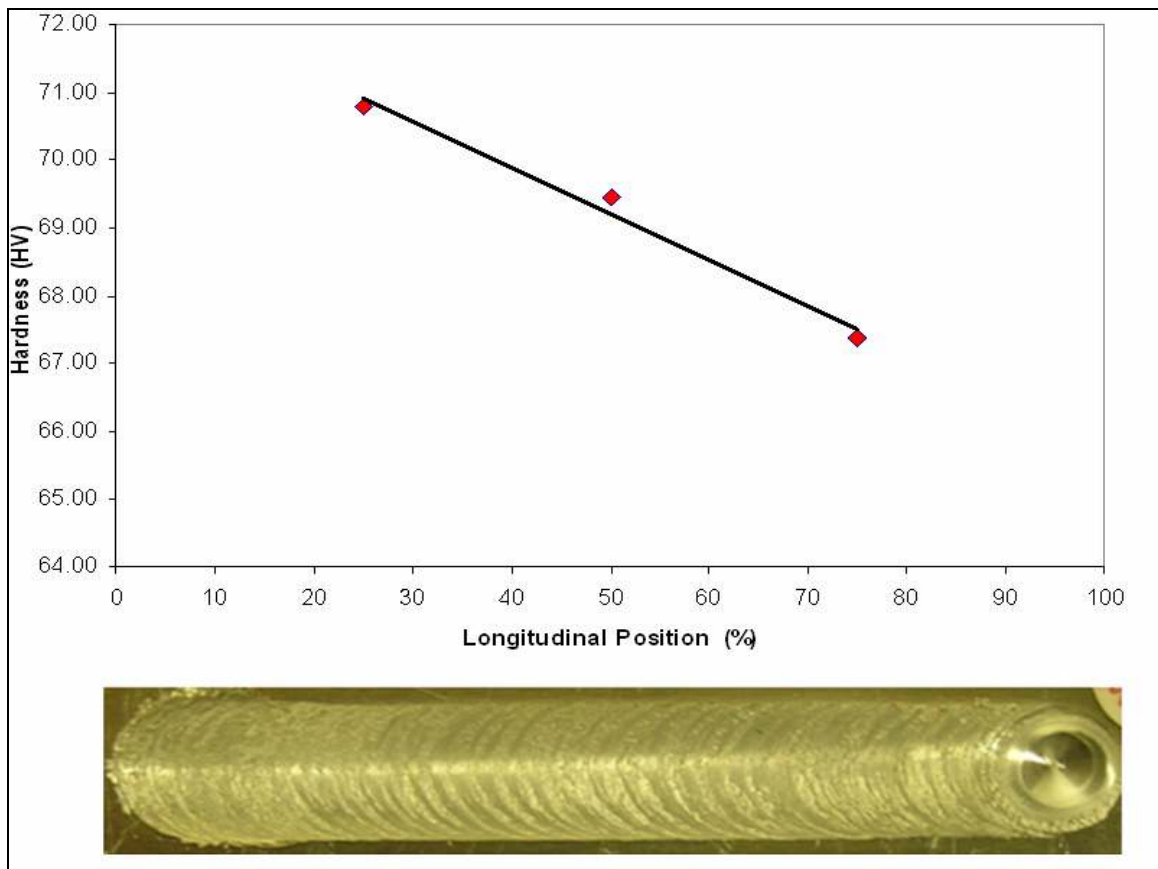


Figure 3- 13 Average hardness (HV) of FS processed at different longotidunal positions (FS processed at 500 rpm and 2 in/min.)

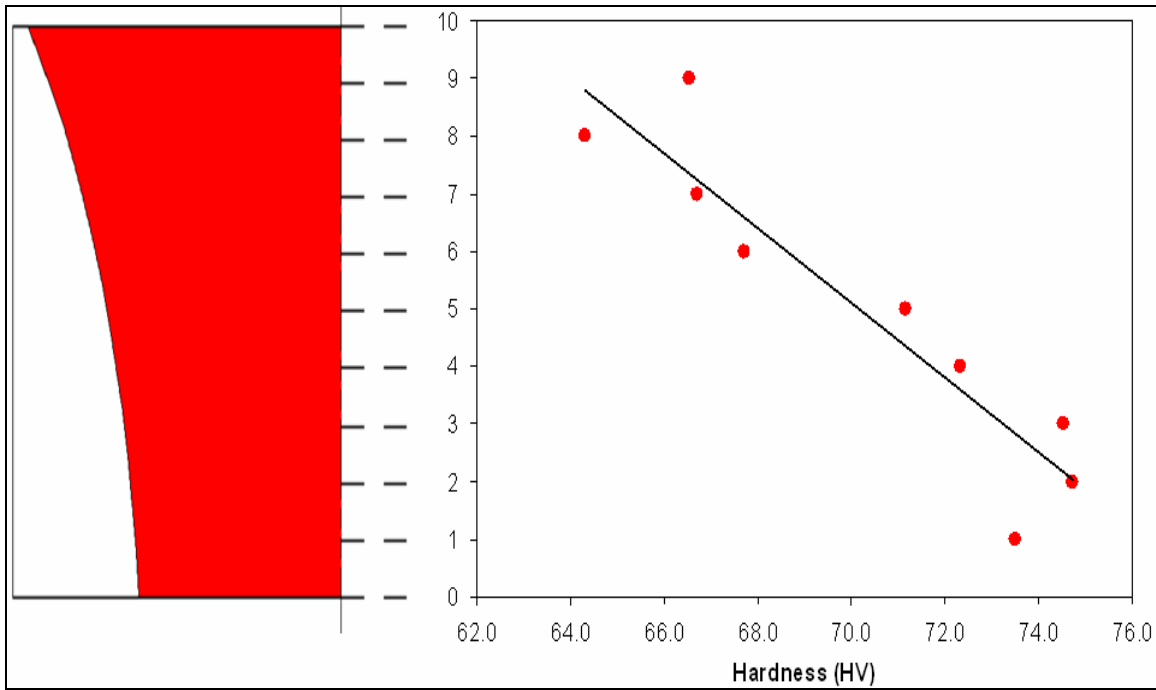


Figure 3- 14 Average hardness (HV) of FS processed at different positions within the (FS processed at 500 rpm and 2 in/min.)

Figure 3-15 shows the hardness profile at a transverse section of AA5052 sample FS processed at 500 rpm and 2.0 in/min. The hardness profile shows that the hardness values at the center of the deformation zone (nugget zone) is higher than the other zones, and as going farther from the nugget the hardness decreases till it reaches its minimum value at edge of the deformation zone (heat affected zone) and then increases again. These results agree with those in the literature such as the results presented by Denquin et al. [38].

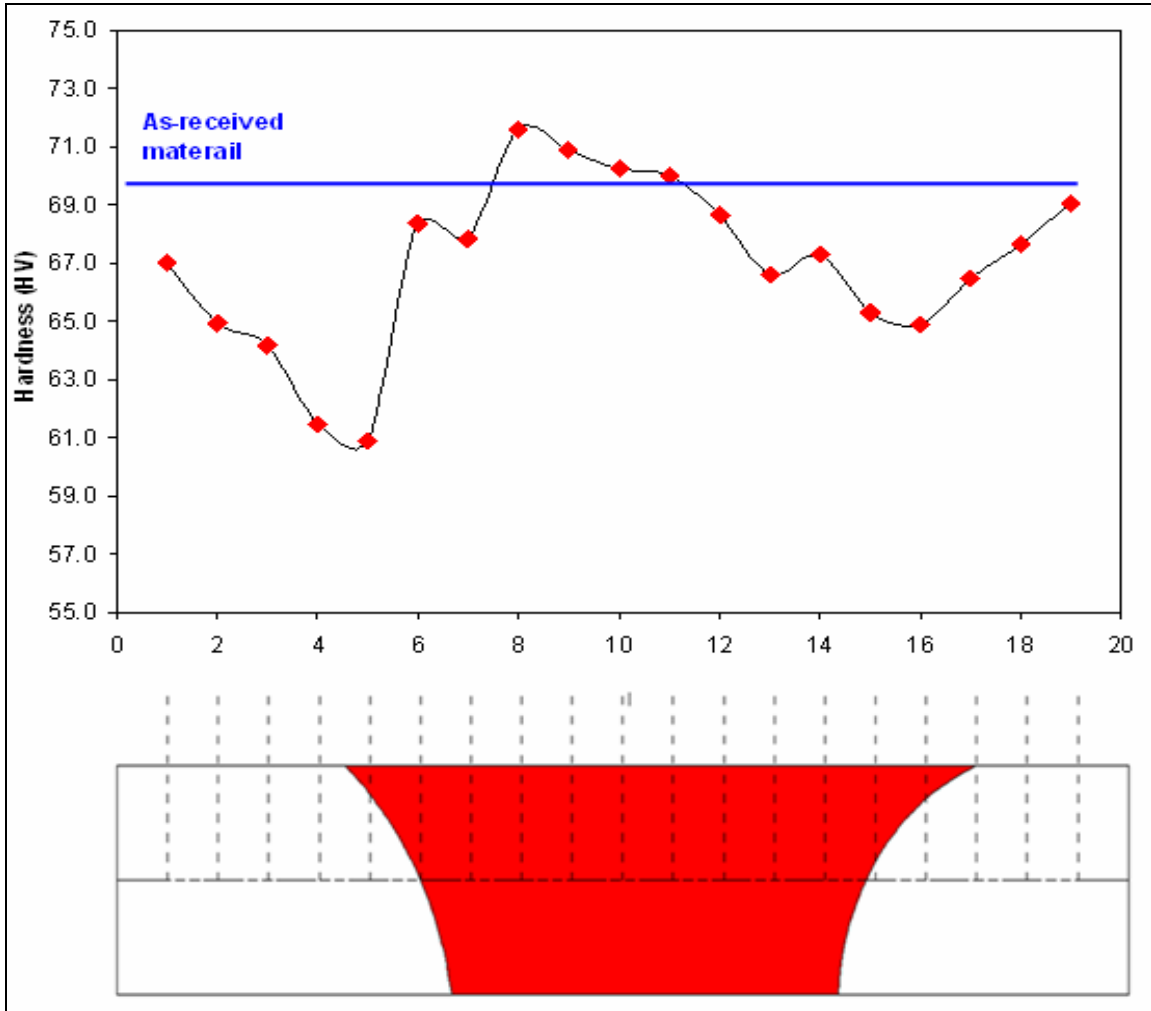


Figure 3- 15 Average hardness (HV) of FS processed at different transvers positions (FS processed at 500 rpm and 2 in/min.)

3.3-3 FS processed quality

The effects of rotational and translational speed on the surface quality of the FS processed material were also investigated. Table 3-3 shows the surface quality AA5052 samples of FS processed at different rotational speed (400-800 rpm). The tool that was used here has $\frac{1}{4}$ " pin diameter, $\frac{1}{8}$ " pin height and $\frac{1}{2}$ " shoulder diameter with no threads on the pin and no concavity on the shoulder. In general, as the rotational speed decreases, the roughness of the surface increases. Also it observed that as increasing the rotational

speed more material is removed and defects appears on the surface. The effects of translational speed are shown in Table 3-4. Generally, as the translational speed increases the roughness of the surface and the amount of the material removed increase. Also, as the translational speed increases, defects on the surface are observed.

Table 3- 3 FS processed AA5052 sheet at different rotational speed

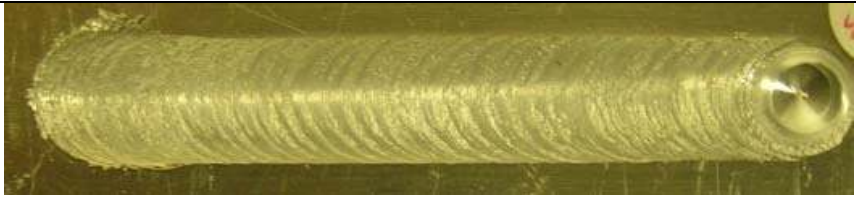
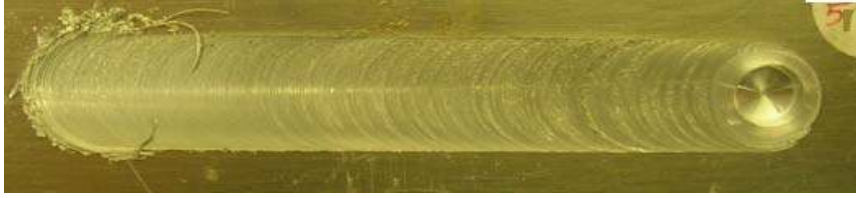

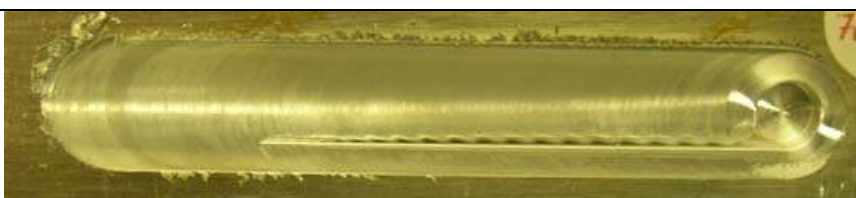




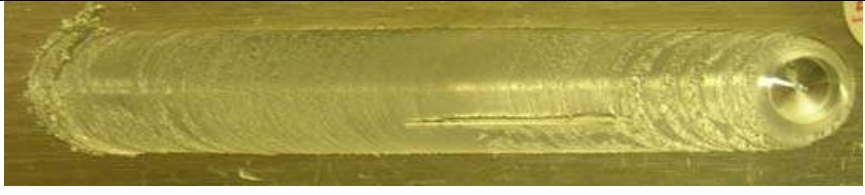
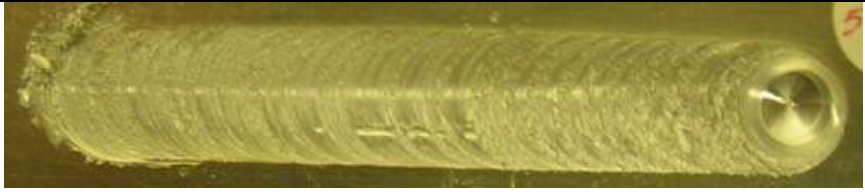
	0.50" shoulder diameter, no threads and no concavity
400 rpm 2.0 in/min.	
500 rpm 2.0 in/min.	
600 rpm 2.0 in/min.	
700 rpm 2.0 in/min.	
800 rpm 2.0 in/min.	

Table 3- 4 FS processed AA5052 sheet at different translational speed

	0.50" shoulder diameter, no threads and no concavity
500 rpm 1.0 in/min.	
500 rpm 1.5 in/min.	
500 rpm 2.0 in/min.	
500 rpm 2.5 in/min.	
500 rpm 3.0 in/min.	

CHAPTER-4 MODELING OF FRICTION STIR PROCESS

Recently Friction Stir Processing (FSP) has become an efficient tool for homogenizing and refining the grain structure of metal sheet. One of the most important issues that hinder the wide spread use of friction stir processing is the lack of predictive models or tools that can predict the microstructure and properties of the processed material so that one can choose the suitable process parameters and achieve the desired microstructure, and optimize the process itself.

Most of the work that has been done in the field of friction stir modeling deal with welding. Very limited work has been done in the field of processing. Different types of modeling work has been done; most of them focus on thermal modeling which deals with the heat generated and temperature history and distribution, others proposed mechanical models that deal with stress, strain and generated forces [17-32]. Limited work has been done to developed coupled thermo-mechanical models that combine mechanical and thermal aspects of the process. Another part of modeling is; the microstructural modeling which aims on microstructural issues such as grain size, void fractions, dislocations etc...But the there are very limited modeling works that combined mechanical, thermal and microstructural parts of the process. The modeling approach presented in this work combines mechanical, thermal and microstructural modeling; it aims at using mechanical modeling to predict the resulting microstructure mainly the grain size from process parameters (rotational and translational speeds) using mechanical and thermal modeling.

The main goal of this work is to develop a new model based on theory and experiments which can predict the resulting grain size of the friction stir processed material, as well as the required power to achieve this grain size. The inputs of this model will be material properties, sheet thickness, FSP tool geometry, and rotational and translational speeds. The main outputs of the model will be the resulting grains size.

4.1 Modeling approach

The modeling approach proposed is a physics-based model that is based on experiments and theory. The main aim of the model is to predict the resulting grain size of the friction stir processed material from the process parameters (rotational and translational speeds), through correlating the resulting grain size with the Zener-Holloman parameter. A brief description of the model is described in the flow chart shown in Figure 4.1. The deformation zone of the friction stir processed material is defined, and then the relation between the tool and material velocities is defined within the deformation zone by defining the contact state variable, and so the velocity fields within the deformation zone are determined. From the velocity fields the strain rate distribution is determined. Using the effective strain rate and the temperature distribution, the Zener-Holloman parameter can be determined. Based on experimental microstructural results, a correlation between the resulting grain sizes and the Zener-Holloman parameter will be developed. In this work, preliminary modeling results of strain rate distribution and strain distribution is presented.

4.1-1 Assumptions

The assumptions used in the proposed model are as follows:

- 1) Only two incompressible flow fields that are combined to describe the material flow in friction stir welds are; rigid body rotation motion and uniform translation motion which were describe in [23].
- 2) The material movement in z-dir (vortex) is not considered.
- 3) The deformation zone has a conical shape. This assumption is based on experimental observations.
- 4) There is a perfect (100%) sticking condition at the interface between the pin of the tool and the material which means that the material velocity there is equal to the tool velocity.

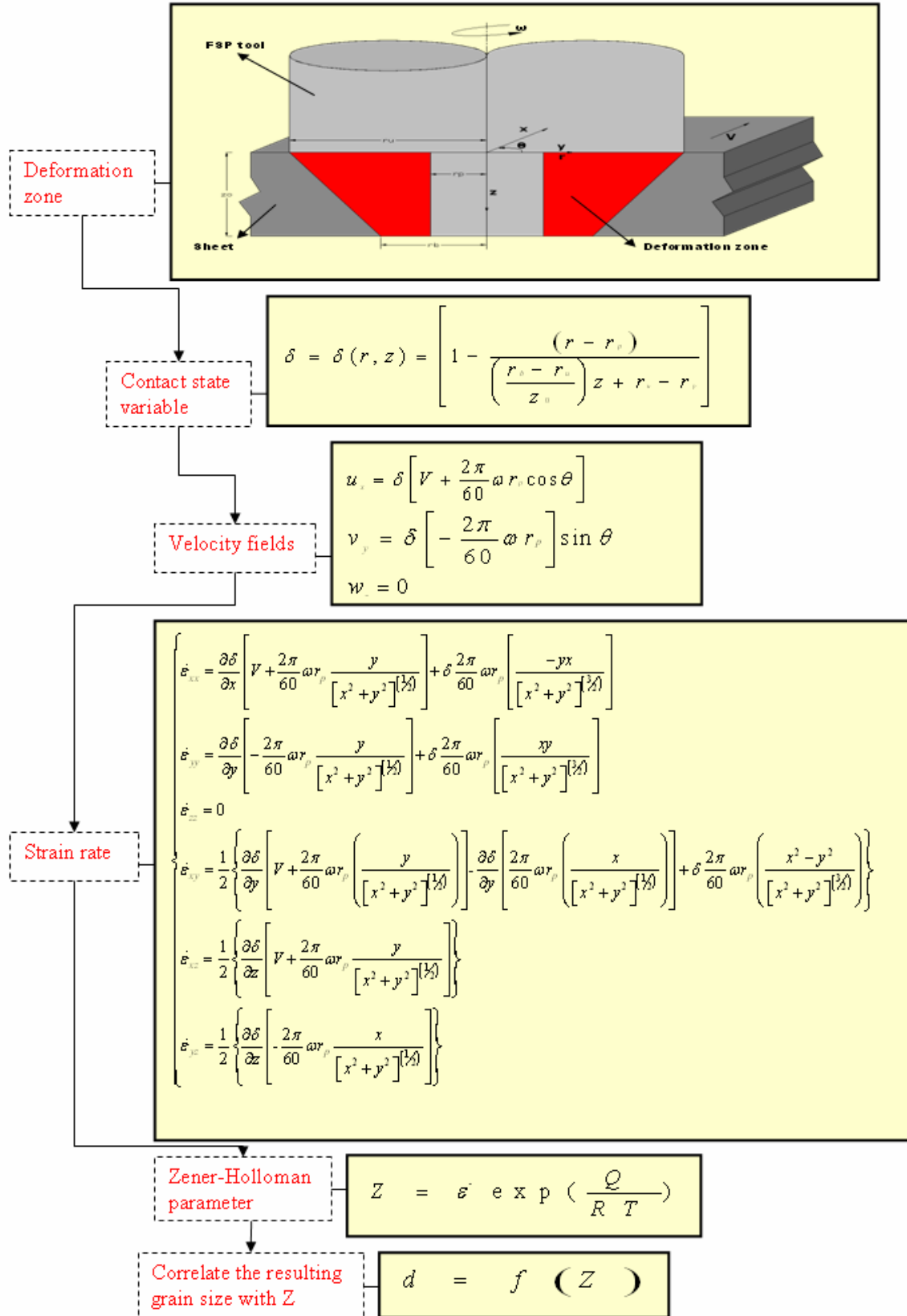


Figure 4- 1 Model flow chart

- 5) The material velocity at the outer edge of the deformation zone is equal to zero.
- 6) The contact state variable changes linearly with the distance from the center of the pin.
- 7) The effect of the shoulder on the mechanical deformation is not included in this model, and the shoulder is assumed to be a source of heat only.
- 8) The effect of threads of the pin is neglected for the time being.

4.1-2 Deformation zone

The first stage in setting up the mechanical model is to define the deformation zone within the friction stir processed material. Based on experimental observations the deformation zone within the thickness of the processed material is assumed to have a semi-conical shape. Figure 4-2 shows a schematic illustration of the deformation zone within the thickness of friction stir processed material.

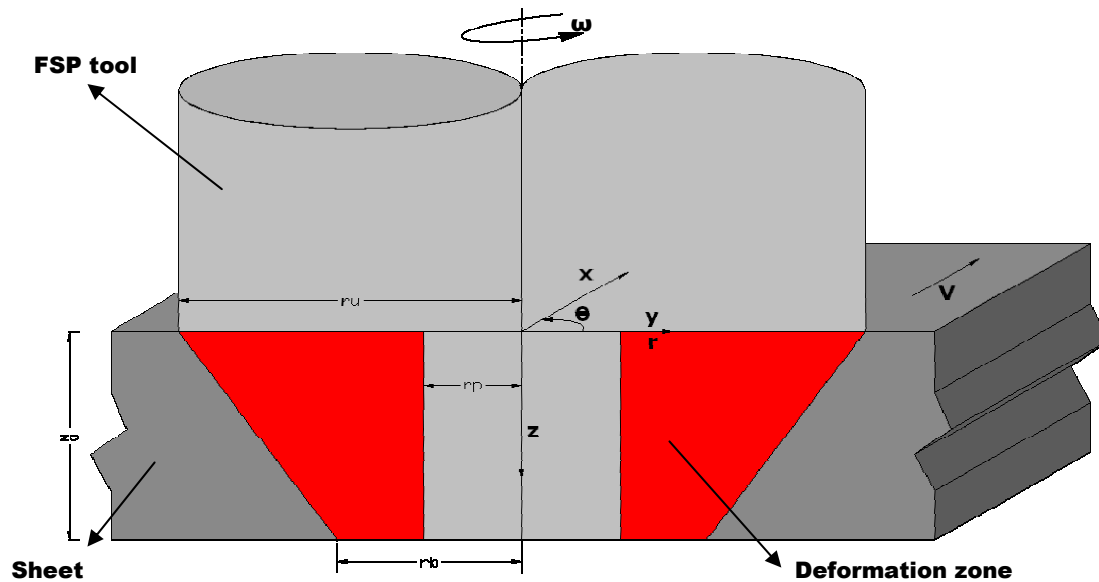


Figure 4- 2 Schematic of FSP deformation zone

4.1-3 Contact state variable

A contact state variable (δ) which relates the material velocity to the tool velocity is introduced [13]. A 100% sticking condition at the pin/material interface is assumed which means that at $r = r_p$, $V_m = V_t$. The velocity of the material is equal to zero at the outer edge of the deformation zone ($V_m = 0$) as shown in Figure 4-2. The contact state variable (δ) is assumed to change linearly with the distance from the center of the pin. Based on these assumptions and geometrical aspects of the deformation zone, the contact state variable can be expressed as:

$$\delta = \frac{V_{material}}{V_{tool}} \quad (4.1)$$

$$\delta = \delta(r, z) = \left[1 - \frac{(r - r_p)}{\left(\frac{r_b - r_u}{z_0}\right)z + r_u - r_p} \right] \quad (4.2)$$

Where r is a variable that represents the radial distance from the tool center, r_p is the pin radius, r_b and r_u are the radii of the deformation zone at the top and bottom of the sheet respectively, and z_0 is the sheet thickness, all the dimensions are in meters (m).

Transforming the contact state variable relation from cylindrical to Cartesian coordinates, the state contact variable can be expressed as in Equation 4.3, and the partial derivatives of it with respect to x , y and z are shown in Equations (4.4 - 4.6)

$$\delta = \delta(x, y, z) = \left[1 - \frac{(\sqrt{x^2 + y^2} - r_p)}{\left(\frac{r_b - r_u}{z_0}\right)z + r_u - r_p} \right] \quad (4.3)$$

$$\frac{\partial \delta}{\partial x} = -\frac{x[x^2 + y^2]^{(1/2)}}{\left(\frac{r_b - r_u}{z_0}\right)z + r_u - r_p} \quad (4.4)$$

$$\frac{\partial \delta}{\partial y} = -\frac{y[x^2 + y^2]^{(1/2)}}{\left(\frac{r_b - r_u}{z_0}\right)z + r_u - r_p} \quad (4.5)$$

$$\frac{\partial \delta}{\partial z} = \frac{\left(\frac{r_b - r_u}{z_0}\right)\left([x^2 + y^2]^{(1/2)} - r_p\right)}{\left[\left(\frac{r_b - r_u}{z_0}\right)z + r_u - r_p\right]^2} \quad (4.6)$$

4.1-4 Velocity fields

We assumed that only two incompressible flow fields are combined to describe the material flow in friction stir welds; rigid body rotation and uniform translation motions which were described in [23]. In this work the material movement in z-dir (vortex motion) is not considered. The velocity fields as function of tool velocities, contact state variable and the location can be expressed as:

The tangential velocity of the material caused by rotational motion is:

$$V_{\theta(m)} = \frac{2\pi}{60} \omega r_p \delta \quad (4.7)$$

The transitional velocity of the material (in x-dir) caused by translational motion:

$$V_{tran(m)} = V \delta \quad (4.8)$$

The velocity fields in Cartesian coordinate:

$$u = \delta \left[V + \frac{2\pi}{60} \omega r_p \frac{y}{[x^2 + y^2]^{(1/2)}} \right] \quad (4.9)$$

$$v = \delta \left[-\frac{2\pi}{60} \omega r_p \frac{x}{[x^2 + y^2]^{(1/2)}} \right] \quad (4.10)$$

$$w = 0 \quad (4.11)$$

The partial derivatives of velocities are:

$$\frac{\partial u}{\partial x} = \frac{\partial \delta}{\partial x} \left[V + \frac{2\pi}{60} \omega r_p \frac{y}{[x^2 + y^2]^{(1/2)}} \right] + \delta \frac{2\pi}{60} \omega r_p \left[\frac{-yx}{[x^2 + y^2]^{(3/2)}} \right] \quad (4.12)$$

$$\frac{\partial u}{\partial y} = \frac{\partial \delta}{\partial y} \left[V + \frac{2\pi}{60} \omega r_p \frac{y}{[x^2 + y^2]^{(1/2)}} \right] + \delta \frac{2\pi}{60} \omega r_p \left[\frac{1}{[x^2 + y^2]^{(1/2)}} - \frac{y^2}{[x^2 + y^2]^{(3/2)}} \right] \quad (4.13)$$

$$\frac{\partial u}{\partial z} = \frac{\partial \delta}{\partial z} \left[V + \frac{2\pi}{60} \omega r_p \frac{y}{[x^2 + y^2]^{(1/2)}} \right] \quad (4.14)$$

$$\frac{\partial v}{\partial x} = \frac{\partial \delta}{\partial x} \left[-\frac{2\pi}{60} \omega r_p \frac{x}{[x^2 + y^2]^{(1/2)}} \right] - \delta \frac{2\pi}{60} \omega r_p \left[\frac{1}{[x^2 + y^2]^{(1/2)}} - \frac{x^2}{[x^2 + y^2]^{(3/2)}} \right] \quad (4.15)$$

$$\frac{\partial v}{\partial y} = \frac{\partial \delta}{\partial y} \left[-\frac{2\pi}{60} \omega r_p \frac{x}{[x^2 + y^2]^{(1/2)}} \right] + \delta \frac{2\pi}{60} \omega r_p \left[\frac{yx}{[x^2 + y^2]^{(3/2)}} \right] \quad (4.16)$$

$$\frac{\partial v}{\partial z} = \frac{\partial \delta}{\partial z} \left[-\frac{2\pi}{60} \omega r_p \frac{x}{[x^2 + y^2]^{(1/2)}} \right] \quad (4.17)$$

$$\frac{\partial w}{\partial x} = \frac{\partial w}{\partial y} = \frac{\partial w}{\partial z} = 0 \quad (4.18)$$

4.1-5 Strain rate fields

With the velocity fields determined, the strain rate at any point within the deformation zone can be determined. The strain rate is calculated from the strain rate-velocity relations (Equation 4.19). The strain rate components of the material within the deformation zone are determined to be as shown in Equations 4.20-4.25. These strain rate components are combined in the strain rate tensor.

Using the strain rate-velocity relations:

$$\dot{\epsilon}_{ij} = \frac{1}{2} \left[\frac{\partial u_i}{\partial x_j} + \frac{\partial u_j}{\partial x_i} \right] \quad (4.19)$$

Then the strain rate fields are:

$$\dot{\epsilon}_{xx} = \frac{\partial \delta}{\partial x} \left[V + \frac{2\pi}{60} \omega r_p \frac{y}{[x^2 + y^2]^{(1/2)}} \right] + \delta \frac{2\pi}{60} \omega r_p \left[\frac{-yx}{[x^2 + y^2]^{(3/2)}} \right] \quad (4.20)$$

$$\dot{\epsilon}_{yy} = \frac{\partial \delta}{\partial y} \left[-\frac{2\pi}{60} \omega r_p \frac{y}{[x^2 + y^2]^{(1/2)}} \right] + \delta \frac{2\pi}{60} \omega r_p \left[\frac{xy}{[x^2 + y^2]^{(3/2)}} \right] \quad (4.21)$$

$$\dot{\epsilon}_{zz} = 0 \quad (4.22)$$

$$\dot{\epsilon}_{xy} = \frac{1}{2} \left\{ \frac{\partial \delta}{\partial y} \left[V + \frac{2\pi}{60} \omega r_p \left(\frac{y}{[x^2 + y^2]^{(1/2)}} \right) \right] - \frac{\partial \delta}{\partial x} \left[\frac{2\pi}{60} \omega r_p \left(\frac{x}{[x^2 + y^2]^{(1/2)}} \right) \right] + \delta \frac{2\pi}{60} \omega r_p \left(\frac{x^2 - y^2}{[x^2 + y^2]^{(3/2)}} \right) \right\} \quad (4.23)$$

$$\dot{\epsilon}_{xz} = \frac{1}{2} \left\{ \frac{\partial \delta}{\partial z} \left[V + \frac{2\pi}{60} \omega r_p \frac{y}{[x^2 + y^2]^{(1/2)}} \right] \right\} \quad (4.24)$$

$$\dot{\epsilon}_{yz} = \frac{1}{2} \left\{ \frac{\partial \delta}{\partial z} \left[-\frac{2\pi}{60} \omega r_p \frac{x}{[x^2 + y^2]^{(1/2)}} \right] \right\} \quad (4.25)$$

4.1-6 Effective strain rate

The effective strain rate according to Von-Mises criteria can be calculated according to equations 4-26:

$$\dot{\epsilon}_{eff} = \sum \left[\frac{2}{3} (\dot{\epsilon}_{ij})^2 \right]^{(1/2)}$$

$$\dot{\epsilon}_{eff} = \left[\frac{2}{3} (\dot{\epsilon}_{xx}^2 + \dot{\epsilon}_{yy}^2 + \dot{\epsilon}_{zz}^2 + 2\dot{\epsilon}_{xy}^2 + 2\dot{\epsilon}_{xz}^2 + 2\dot{\epsilon}_{yz}^2) \right]^{(1/2)} \quad (4.26)$$

4.1-7 Zener-Holloman parameter

Friction stir processing is considered to be a hot working process which means that the flow stress is dependent on the strain rate and the working temperature. Since the resulting grains is dynamically recrystallized and mainly depend on the flow stress, it is useful to use the Zener-Holloman parameter which combines the effects of strain rate and temperature together in a single parameter to relate the resulting grain size of friction stir processed material to Zener-Holloman parameter. During the high temperature deformation the superposition of work hardening and work softening leads to a competitive shrinkage and growth of subgrains [29]. So the resulting grain structure depends on the imposed deformation conditions like temperature and strain rate.

Using temperature distribution and the calculated effective strain rate the Zener-Holloman parameter can be determined. Since the working temperature and the strain rate have a great influence on the resulting grain size, and the Zener-Holloman parameter which is a function of the working temperature and the effective strain rate so it is possible to develop a correlation to predict the resulting grain size using the Zener-Holloman parameter.

$$Z = \dot{\epsilon} \exp\left(\frac{Q}{RT}\right) \quad (4.27)$$

Where $\dot{\epsilon}$ is the strain rate, R is the gas constant, T is the temperature, and Q is the related activation energy is taken place.

4.2 Preliminary results

The effective strain rate within the deformation zone of the processed zone is calculated using the proposed model. As expected the results shows that the strain rate directly proportional to the rotational speed of the tool and show good agreement in the trend with the work done by Chang et al. [18] (Figure 4-3). The effect of the translational speed is almost neglected compared to the effect of the rotational speed and this is shown in Figure 4-4. The main reason for this is that the translational speed is relatively small compared to the rotational speed.

The preliminary modeling results show that the strain rate decreases as the radial distance from the tool center increases (Figure 4-5). There are some variations in the strain rate values at different angles, as shown in Figure 4-6. The strain rate is higher at the advancing side ($\theta = 0^\circ$) than that at the retreating side ($\theta = 180^\circ$). The strain rate increases going from top to the bottom in the sheet (Figure 4-7).

Effective strain rate vs. rotational speed

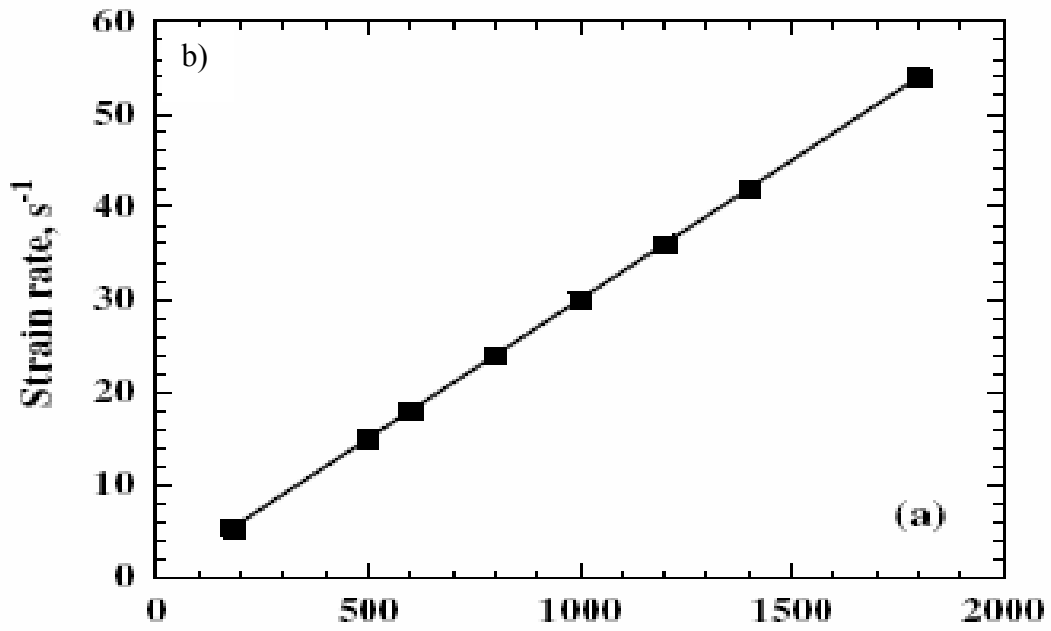
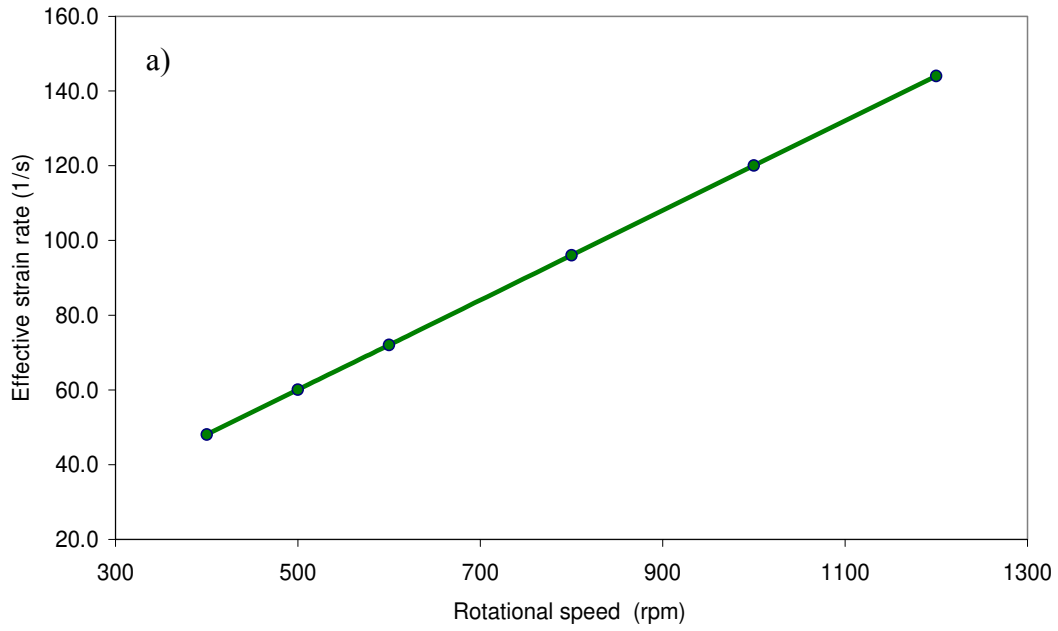


Figure 4- 3 The effect of rotational speed on the effective strain rate (a) result from the proposed model and (b) result from literature [18].

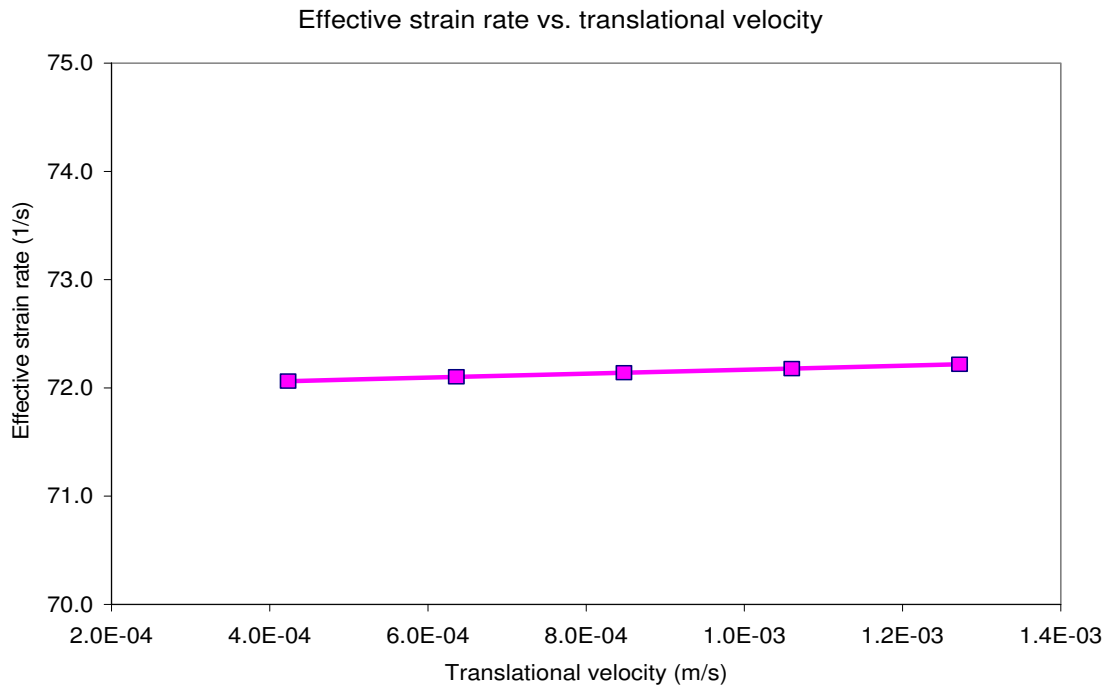


Figure 4- 4 The effect of translational speed on the effective strain rate (modeling results).

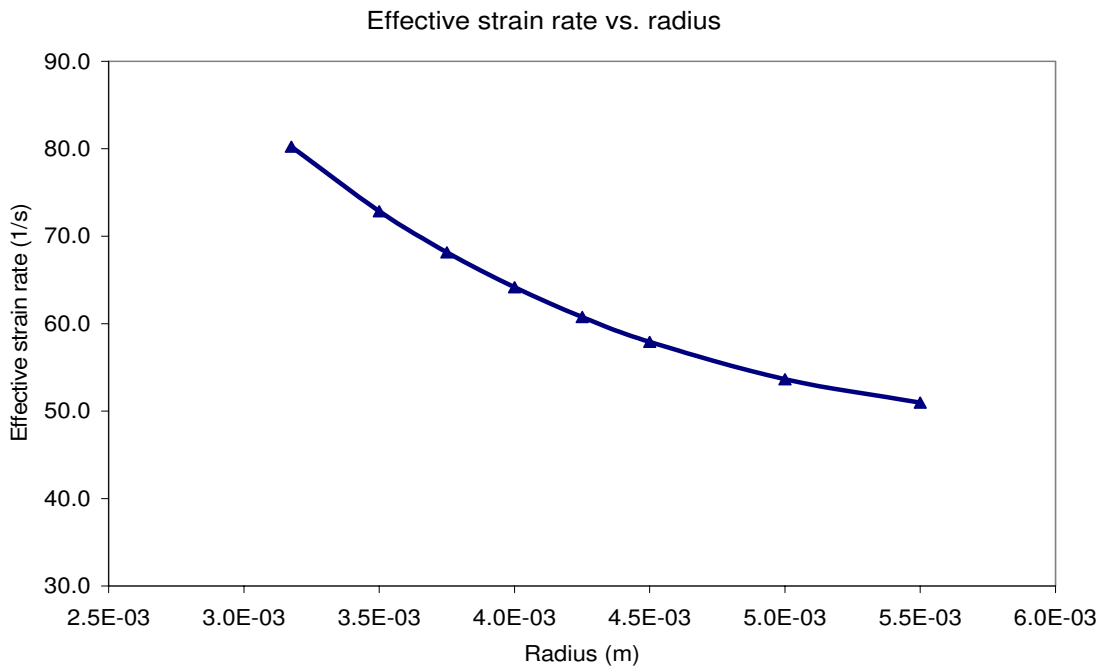


Figure 4- 5 The variation of effective strain rate with the distance from the center of the tool (modeling results).

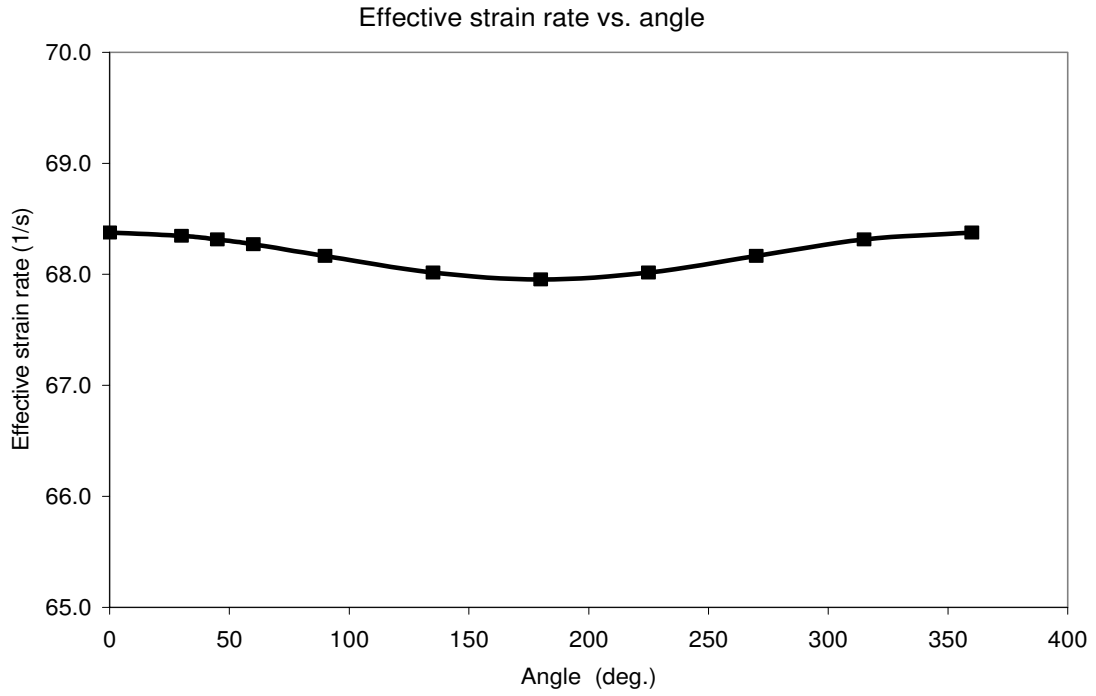


Figure 4- 6 The variation of effective strain rate with the angle (modeling results).

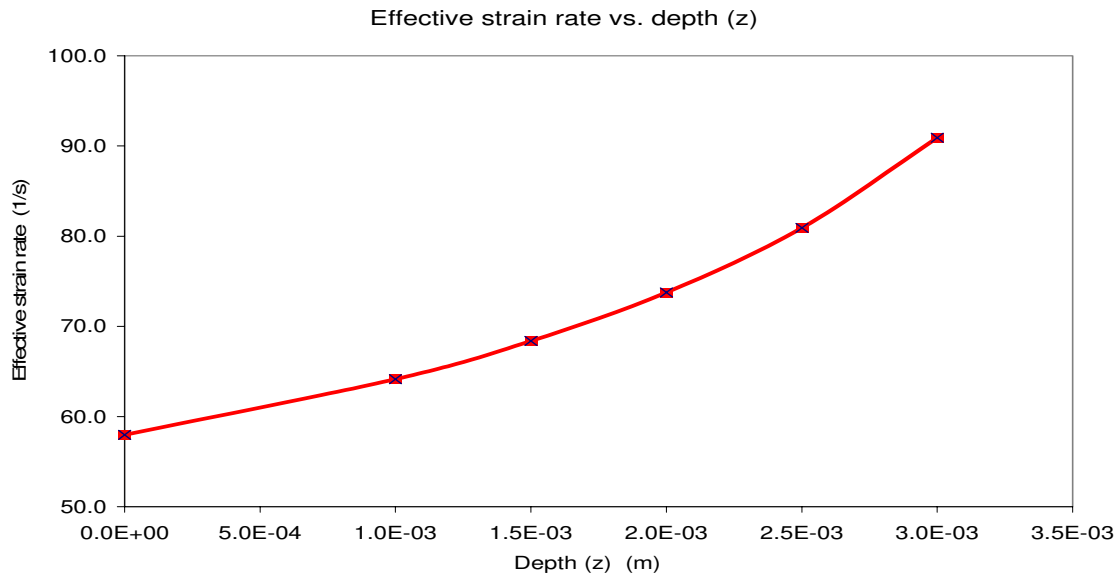


Figure 4- 7 The variation of effective strain rate with the depth within the sheet thickness (modeling results).

The strain rate distribution within the deformation zone is calculated using a MATLAB code. It is assumed that the strain rate values are the same for the region occupied by the pin ($r < r_p$). Figures 4-8 to 4-10 show the strain rate distributions within the deformation zone at different rotational speeds (400-800 rpm). As expected, it is obviously shown that as the rotational speed increases the strain rate increases. Comparing Figures 4-9 and 4-11, show that the effect of translational speed is negligible when considering the strain rate distribution (Figure 4-9 and 4-11 show strain rate distribution at 600 rpm and 2 and 4 in/min.).

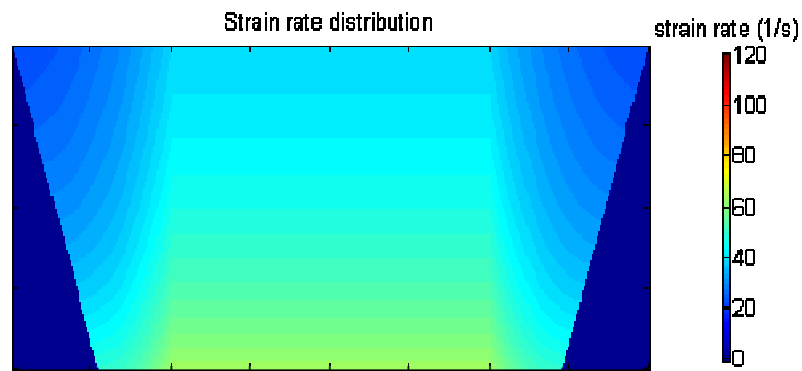


Figure 4- 8 The strain rate distributions within the deformation zone at 400 rpm and 2.0 in/min. (modeling results using MATLAB).

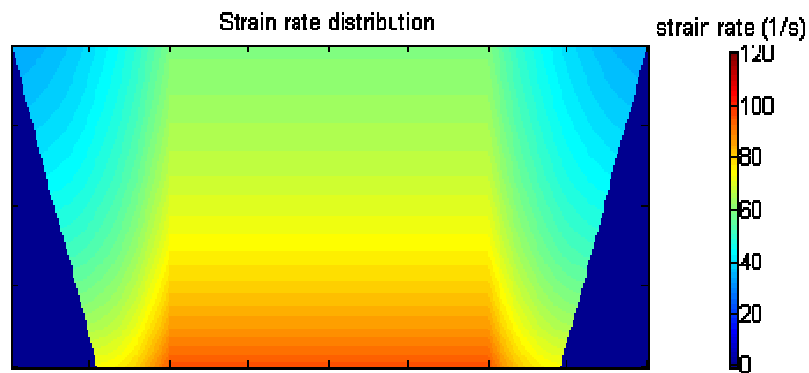


Figure 4- 9 The strain rate distributions within the deformation zone at 600 rpm and 2.0 in/min. (modeling results using MATLAB).

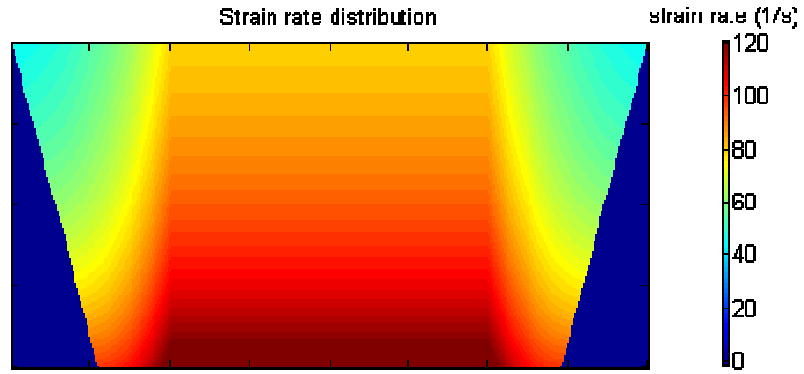


Figure 4- 10 The strain rate distributions within the deformation zone at 800 rpm and 2.0 in/min.
(modeling results using MATLAB).

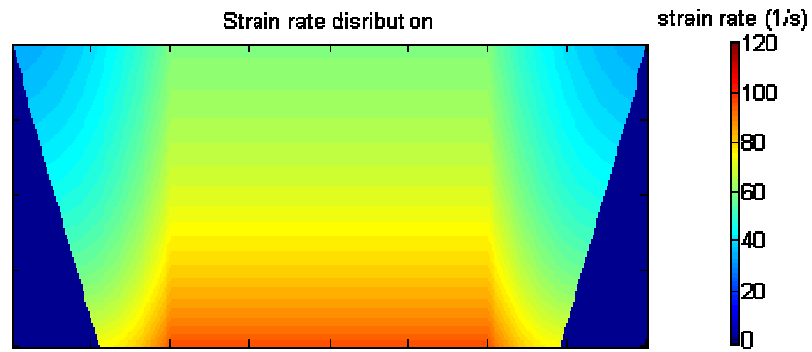


Figure 4- 11 The strain rate distributions within the deformation zone at 600 rpm and 4.0 in/min.
(modeling results using MATLAB).

CHAPTER-5 SUMMARY AND FUTURE WORKS

Friction stir processing is an effective microstructural modification process that produces very fine and homogenous grain structure. The results for FSP commercial Aluminum alloy 5052, shows that a significant grain refinement is obtained using FSP and not only the grains are finer but the grain structure is more homogenous. Generally, smaller grain sizes are obtained at lower rotational speeds, but the effect of translational speed is not significant on the resulting grain size.

The results shows that the hardness of the material is affected by FSP, and at certain combinations of rotational and translational speeds the hardness of the FS processed area is even higher than that of the original material. It is observed that the hardness of FS processed area increases as the rotational speed decreases, and as the translational speed increases. The results of the hardness profiles show that the hardness has higher values at the bottom of the processed zone, and the hardness values are less at the edge of the processed zone. These observations suggested that the generated heat has significant influence on the resulting hardness.

A new modeling approach is proposed in this work. The main aim of the model is to predict the resulting grain size of the friction stir processed material from the process parameters (rotational and translational speeds), through correlating the resulting grain size with the Zener-Holloman parameter. Briefly, the deformation zone is defined based on experimental observations, and then the relation between the tool and material velocities is defined within that zone. The velocity fields within the deformation zone are then determined. From the velocity fields the strain rate distribution is determined. Using the effective strain rate and the temperature distribution, the Zener-Holloman parameter can be determined. Based on experimental microstructural results, a correlation between the resulting grain sizes and the Zener-Holloman parameter will be developed.

Results of effective strain rate distribution within the deformation zone are presented in this work. These results show that effective strain rate increases as the rotational speed increases, but the effect of translational speed is negligible compared to the effect of rotational speed. It is also shown that as going farther from the center of the FSP tool the effective strain rate decreases, and the strain rate values increase as going from top to bottom within the thickness of the deformation zone.

5.1 Future work

This study shows that FSP has the potential to be one of the most effective techniques for microstructural modification. But the lack of data and accurate models hinder the widespread use of FSP. In this work a modeling approach to predict the grain size is proposed, and more work has to be done in this area. The following are planned to be done:

- Finding the temperature distribution during the process and incorporating the temperature distribution into our model to determine the Zener-Holloman parameter, and correlate it to the resulting grain size.
- Considering the motion in z-direction (vortex motion) within the deformation in our model.
- Considering the effect of shoulder on the mechanical deformation
- More investigation on the contact state variable; its values at different conditions, material and position and how it varies.
- Predict the generated forces, torque and power.
- More experimental work has to be done to investigate the effect of tool design on the process and the resulting microstructure.
- Measure the generated forces and torque, and compare to the predicted results as well as try to correlate them to the resulting microstructure.
- Use different techniques; such as thermocouples and infrared technology to determine the temperature distributions during the process.

- Investigate the effect of cooling rate on the process as well as on the resulting microstructure.
- Investigate overlapped multi-passes to process a whole sheet of material
- Design new experiment to investigate the potential of FSP as crack repairing technique.

REFERENCES

1. Thomas, E.D. Nicholas, J.C. Needham, M.G. Murch, P. Temlesmith, C.J. Dawes. GB Patent Application No. 9125978.8, December 1991.
2. C.J. Dawes, W.M. Thomas: Annual North American Welding Research Conference 1995, p. 301.
3. R. Johnson and S. Kallee, "Friction Stir Welding". *Materials World*, Vol. 7 no. 12 pp. 751-53 December 1999.
4. J. Su, T. Nelson and C. Sterling. "Friction stir processing of large-area bulk UFG aluminum alloys". *Scripta Materialia* 52 (2005) pp.135-140.
5. M. Peel, A. Steuwer, M. Preuss and P. Withers. "Microstructure, mechanical properties and residual stresses as a function of welding speed in aluminum AA5083 friction stir welds", *Acta Materialia*, Volume 51, Issue 16, (2003), pp. 4791-4801.
6. M. Sutton, B. Yang, A. Reynolds and R. Taylor. "Microstructural studies of friction stir welds in 2024-T3 aluminum". *Materials Science and Engineering A323* (2002) pp. 160-166.
7. M. Mahoney, W. Bingel, S. Sharma and R. Mishra. "Microstructural modification and resultant properties of friction stir processed Cast NiAl Bronze". *Material Science Forum* Vols. 426-432 (2003) pp. 2843-2848.
8. K. Jata and S. Semiatin. "Continuous dynamic recrystallization during friction stirs welding of high strength aluminum alloys". *Scripta Materialia*, Volume 43, Issue: 8, pp.743-749.
9. S. Benavides, Y. Li, L. E. Murr, D. Brown and J. McClure. "Low-temperature friction-stir welding of 2024 aluminum", *Scripta Materialia*, Vol. 41, Issue 8, (September 1999) pp. 809-815.
10. Y. Kwon, I. Shigematsu and N. Saito. "Mechanical properties of fine-grained aluminum alloy produced by friction stir process". *Scripta Materialia* 49 (2003) pp. 785-789.
11. R. Itharaju and M. Khraisheh. "On the forces generated during friction stir processing of aluminum 5052 sheets". *Ultrafine Grained Material III TMS*, 2004.

12. R. Mishra, L. Johannes, I. Charit and A. Dutta. "Multi-pass friction stir superplasticity in aluminum alloys". Proceedings of (2005) NSF.
13. Z. Ma, R. Mishra and M. Mahoney. "Superplasticity in cast A356 induced via friction stir processing". Scripta Materialia 50 (2004) pp. 931-935.
14. H. Salem, A. Reynolds and J. Lyons. "Microstructure and retention of superplasticity of friction stir welded superplastic 2095 sheet", Scripta Materialia, (March 2002), Vol. 46, Issue 5, pp. 337-342.
15. I. Charit, R. Mishra. "High strain rate superplasticity in a commercial 2024 Al alloy via friction stir processing" Materials Science and Engineering A, Volume 359, Issues 1-2, 25 (October 2003), pp. 290-296.
16. Z. Ma, R. Mishra and M. Mahoney. "Superplastic deformation behavior of friction stir processed 7075Al alloy" Acta Materialia, (October 2002), Volume 50, Issue 17, pp. 4419-4430.
17. A. Dutta, I. Charit, L. Johannes and R. Mishra. "Deep cup forming by superplastic punch stretching of friction stir processed 7075 Al alloy". Materials Science and Engineering A395 (2005) pp. 173-179.
18. P. Ulysse "Three-dimensional modeling of friction stir-welding process". International Journal of Machine Tools and Manufacture 42 (2002) pp. 1549-1557.
19. C. Chang, C. Lee and J. Huang. "Relationship between grain size and Zener-Holloman parameter during friction stir processing in AZ31 Mg alloys". Scripta Materials (2004).
20. P. Heurtier, C. Desrayaud and F. Montheillet. "A thermomechanical analysis of the friction stir welding process". Materials Science Forum Vols. 396-402 (2002) pp. 1537-1542.
21. H. Schmidt, J. Hattel and J. Wert. "An analytical model for the heat generation in friction stir welding". Modeling and Simulation in Materials Science and Engineering 12 (2004) pp.143-157.
22. M. Stewart, G. Adams, A. Nunes and P. Romine. "A combined experimental and analytical modeling approach to understanding friction stir welding". Developments in theoretical and applied mechanics, vol. XIX, (1998).

23. W. Arbegast. "Modeling friction stir joining as a metal working process". TMS (2003).
24. J. Schneider and A. Nunes. "Thermo-Mechanical Processing in Friction Stir Welds". Friction Stir Welding and Processing II, TMS (2003) pp. 43-51.
25. A. Reynolds, Z. Khandkar, T. Long, W. Tang and J. Khan. "Utility of relatively simple models for understanding process parameter effects on FSW". Materials Science Forum Vols. 426-432 (2003) pp. 2959-2694.
26. L. Fratini and G. Buffa. "CDRX modeling in friction stir welding of aluminum alloys". International Journal of Machine Tools & Manufacture 45 (2005) pp. 1188-1194.
27. C. Chen and R. Kovacevic. "Finite element modeling of friction stir welding – thermal and thermomechanical analysis". International Journal of Machine Tools and Manufacture 43 (2003) pp. 1319-1326.
28. M. Song and R. Kovacevic. "Thermal modeling of friction stir welding in a moving coordinate system and its validation". International Journal of Machine Tools and Manufacture 43 (2003) pp. 605-615.
29. P. Dong F. Lu, J. Hong and Z. Cao. "Coupled thermomechanical analysis of friction stir welding process using simplified models". Science and Technology of Welding and Joining (2001) Vol. 6 No.5, pp 281-287.
30. A. Askari, S. Silling, B. London and M. Mahoney. "Modeling and analysis of friction stir welding processes". Friction Stir Welding and Processing, TMS (2001), pp. 4354.
31. S. Xu, X. Deng A. Reynolds and T. Seidel. "Finite element simulation of material flow in friction stirs welding". Science and Technology of Welding and Joining, Vol. 6 No. 3 (2001) pp. 191-193.
32. C. Chen and R. Kovacevic. "Thermomechanical modeling and force analysis of friction stir welding by the finite element method". Proc. Instn. Mech. Engrs Vol. 218 Part C: J. Mechanical Engineering Science (2004) pp. 17-33.
33. Dr. Riederer Verlag, edited by Frank Haessner. "Recrystallization of metallic materials ". Second edition (1978).

34. ASM Handbook, Vol. 2 Properties and selection: Nonferrous Alloys and Special Purpose Material. ASM International (1992) p. 62.
35. A.P. Zhilyaev et al.: Scripta Materialia 46 (2002), p. 575.
36. Y.S. Sato, M. Urata, H. Kokawa and K. Ikeda. "Hall-Petch relationship in friction stir welds of equal channel angular-pressed aluminum alloys". Materials Science and Engineering A354 (2003) pp. 298-305.
37. M. Guerra, C. Schmidt, J. McClure, L. Murr and A. Nunes. "Flow patterns during friction stir welding". Materials Characterization, Vol. 49 (2003) pp. 95-101.
38. A. Denquin D. Allehaux, M.-H. Campaganc and G. Lapasset-. "Relationship between microstructural variations and properties of friction stir welded 6056 aluminum alloy". Welding in the World, (2002) pp.14-19.
39. Y.S. Sato, F.Yamashita, Y. Sugiura, S. Hwan, C. Park and H. Kokawa. "FIB-assisted TEM study of an oxide array in the root of friction stir welded aluminum alloy". Scripta Materialia 50 (2004) pp. 356-369.
40. R. S. Mishra, Z.Y. Ma and I. Charit. "Friction stir processing: a novel technique for fabrication of surface composite". Material Science and Engineering A00 (2002) pp. 1-4.
41. Φ . Frigaard, Φ . Grong and O.T. Midling. "A process model for friction stir welding of age hardening Aluminum alloys". Metallurgical and Materials Transactions A Volume 32A, (May 2001) pp. 1189-1200.
42. Colligan. "Material flow behavior during friction stir welding of Aluminum". Supplement to Welding Journal, (July 1999) pp. 229s-237s.
43. K. V. Jata, K. K. Sankaran and J.J. Ruschau. "Friction-stir welding effects on microstructure and fatigue of aluminum alloy 7075-T7451". Metallurgical and Materials Transactions A, Vol. 31A (Sept. 2000) pp. 2181-2192.
44. M. Song and R. Kovacevic. "Numerical and experimental study of the heat transfer process in friction stir welding". Proc. Instn. Mech. Engrns Vol.217 Part B: J. Engineering Manufacture. (2003) pp. 17-33.
45. T. W. Nelson, R. G. Steel and W. J. Arbegast. "In situ thermal studies and post-weld mechanical properties of friction stir welds in age hardenable aluminum".

- Science and Technology of Welding and Joining, Vol. 8 No. 4 (2003) pp. 283-288.
46. W. M. Thomas and G. Sylva. "Developments in friction stir welding". Proceeding of Joining of Advanced and Specialty Materials 13-15 October 2003, ASM international (2004) pp. 59-66.
 47. M. Adams-Hughes, P. Kalu, M. Khraisheh and N. Chandra. "Microcharacterization and Texture analysis of friction stir processed AA5052 alloy" Friction Stir Welding and Processing III, TMS annual meeting (2005) pp. 3-10.
 48. M. Khraisheh, B. Darras, P. Kalu, M. Adams-Hughes and N.Chandra "Correlation between the microstructure and forces generated during friction stir processing of AA5052" Materials Science Forum Vols. 475-479 (2005) pp. 3043-3046.

VITA

Date and Place of Birth

- May 28th, 1978 in Amman, Jordan

Education

- Bachelor's Degree in Mechanical Engineering, University of Jordan, Amman Jordan (2001)

Work Experience

- Mechanical Engineer at Consolidated Consultants Co., Amman, Jordan (August 2001 – July 2003)
- Teaching Assistant and Research Assistant at University of Kentucky, Department of Mechanical Engineering, (from August 2003)

Publications & Presentations

- B. Darras, M. Khraisheh & F. Abu-Farha, "Friction Stir Processing of AZ31 Commercial Magnesium Alloy", Transactions of NAMRI/SME (submitted)
- M. Khraisheh, B. Darras, P. Kalu, M. Adams-Hughes & N. Chandra "Correlation between the microstructure and forces generated during friction stir processing of AA5052", Materials Science Forum Vols. 475-479 (2005) pp. 3043-3046.
- M. Nazzal, M. Khraisheh & B. Darras "Finite Element Modeling and Optimization of Superplastic Forming Using Variable Strain Rate Approach" Journal of Materials Engineering and Performance, Issue (December 2004).
- B. Darras & M. Khraisheh, "Friction Stir Processing: A Tool to Produce Nanocrystalline Sheet Metals", Poster presentation at The International Workshop of Nanomaterials (2004).

- B. Darras & M. Khraisheh , “ Friction Stir Processing”, Presentation at The 3RD International Conference on Structural Stability & Dynamics (June 2005)
- B. Darras, “ Friction Stir Processing”, Presentation at Sustainability Seminar-Center of Manufacturing and Robotics-University of Kentucky (April 2005)